© 2022. Published by The Company of Biologists Ltd | Journal of Experimental Biology (2022) 225, jeb243460. doi:10.1242/jeb.243460

RESEARCH ARTICLE

Insulin-like peptide 3 stimulates hemocytes to proliferate in anautogenous and facultatively autogenous mosquitoes

Ellen O. Martinson*, Kangkang Chen, Luca Valzania‡, Mark R. Brown and Michael R. Strand§

ABSTRACT

Most mosquito species are anautogenous, which means they must blood feed on a vertebrate host to produce eggs, while a few are autogenous and can produce eggs without blood feeding. Egg formation is best understood in the anautogenous mosquito *Aedes aegypti*, where insulin-like peptides (ILPs), ovary ecdysteroidogenic hormone (OEH) and 20-hydroxyecdysone (20E) interact to regulate gonadotrophic cycles. Circulating hemocytes also approximately double in abundance in conjunction with a gonadotrophic cycle, but the factors responsible for stimulating this increase remain unclear. Focusing on *Ae. aegypti*, we determined that hemocyte abundance similarly increased in intact blood-fed females and decapitated blood-fed females that were injected with ILP3, whereas OEH, 20E or heat-killed bacteria had no stimulatory activity. ILP3 upregulated insulin-insulin growth factor signaling in hemocytes, but few genes – including almost no transcripts for immune factors – were differentially expressed. ILP3 also stimulated circulating hemocytes to increase in two other anautogenous (*Anopheles gambiae* and *Culex quinquefasciatus*) and two facultatively autogenous mosquitoes (*Aedes atropalpus* and *Culex pipiens molestus*), but had no stimulatory activity in the obligately autogenous mosquito *Toxorhynchites amboinensis*. Altogether, our results identify ILPs as the primary regulators of hemocyte proliferation in association with egg formation, but also suggest this response has been lost in the evolution of obligate autogeny.

KEY WORDS: Neuropeptide, Insulin-like peptides, Ecdysone, Anautogeny, Autogeny, Immunity

INTRODUCTION

Mosquitoes form a monophyletic assemblage (Diptera: family Culicidae) of more than 3500 species in two subfamilies (Culicinae and Anophilinae) (Harbach and Kitching, 1998; Bertone et al., 2008; Reidenbach et al., 2009). Most mosquitoes are also anautogenous, which means that adult females must blood feed on a human or other vertebrate host to produce eggs that develop from primary follicles in the ovaries (Clements, 1992). Each gonadotrophic cycle is usually activated by a separate blood meal, while successive blood meals underlie how anautogenous mosquitoes can transmit blood-borne pathogens between hosts (Clements, 1992; Briegel, 2003; Fernandes and Briegel, 2005; Attardo et al., 2005). In contrast, some species in the Culicinae are autogenous and can produce eggs without blood feeding (Roubaud, 1929; Rioux et al., 1975).

Regulation of egg formation is best understood in *Aedes aegypti*, which is a primarily anautogenous culicine that transmits several pathogens to humans (Powell and Tabachnick, 2013). When adult females emerge from the pupal stage, each primary follicle consists of an oocyte and nurse cells that are surrounded by somatic follicle cells (Valzania et al., 2019). Primary follicles remain arrested unless a female blood-feeds, which induces neurosecretory cells in the brain to release insulin-like peptides (ILPs) and ovary ecdysteroidogenic hormone (OEH) that bind different but related receptor tyrosine kinases (RTKs) (Strand et al., 2016). ILP and OEH binding to receptors expressed in the ovaries also activates primary follicles (Valzania et al., 2019). ILPs and OEH stimulate follicle cells to produce 20-hydroxyecdysone (20E) (Brown et al., 2008; Vogel et al., 2015) while 20E and ILP signaling interact to induce the fat body to produce vitellogenin and other yolk components 6–30 h post-blood meal (PBM) (Roy et al., 2007; Valzania et al., 2019). Each oocyte packages yolk, followed by follicle cells secreting a chorion, which results in mature eggs that females lay 48–72 h PBM. ILPs and 20E stimulate other anautogenous species such as *Anopheles gambiae* (Anophilinae) to produce eggs (Brown and Cao, 2001; Krieger et al., 2004; Pondeville et al., 2008; Baldini et al., 2013; Nuss et al., 2018). Blood-meal-independent release of ILPs and OEH after adult emergence also stimulates follicle cells to produce 20E, which upregulates vitellogenesis and egg formation in the autogenous mosquito *Aedes atropalpus* (Gulia-Nuss et al., 2012). Thus, the hormones that activate egg formation appear to be fundamentally similar in both anautogenous and autogenous species.

Certain immune responses are also activated by blood feeding as a form of priming or anticipatory defense against potential pathogens (Castillo et al., 2006; Upton et al., 2015; Reynolds et al., 2020). For example, immune cells (hemocytes) in circulation markedly increase in abundance in *Ae. aegypti* and *An. gambiae* after a blood meal, followed by a decline after females oviposit (Castillo et al., 2006; Bryant and Michel, 2014, 2016). ILP3 stimulates hemocytes to proliferate in *Ae. aegypti*, while knockdown of the insulin receptor (IR) by RNA interference (RNAi) disables proliferation (Castillo et al., 2011). In contrast, 20E promotes increased phagocytic activity in hemocytes and upregulates leucine-rich repeat protein 9 (LRIM9) expression in the fat body of *An. gambiae*, while also affecting the expression of certain immune genes in two cell lines established from *An. gambiae* (Muller et al., 1999; Upton et al., 2015; Reynolds et al., 2020). 20E has further been suggested to play a role in blood-meal-associated hemocyte proliferation in *An. gambiae* (Bryant and Michel, 2014).

We thus had two goals in this study. First, we assessed whether only ILPs mediate hemocyte proliferation or whether 20E and OEH also have stimulatory activity. Second, we examined whether

Department of Entomology, University of Georgia, Athens, GA 30602, USA. *Present address: Department of Biology, University of New Mexico, Albuquerque, NM 87131, USA. ‡Present address: Genetics and Developmental Biology Unit, Institut Curie, CNRS UMR 3215, 75248 Paris, France.

§Author for correspondence (mrstrand@uga.edu)

M.R.S., 0000-0003-1844-7460

Received 6 September 2021; Accepted 31 January 2022

hemocyte proliferation in association with egg formation is conserved among mosquitoes or has potentially been lost in autogenous species. Focusing first on *Ae. aegypti*, we report that ILP3 and blood feeding similarly stimulated hemocytes to proliferate, whereas OEH, 20E or systemic infection by bacteria did not. However, almost no immune genes were differentially expressed in hemocytes in response to blood feeding or ILP3. Comparative assays indicated that ILP3 from *Ae. aegypti* but not OEH or 20E also stimulated hemocytes to increase in other anautogenous species including *An. gambiae* and two facultatively autogenous species, but did not do so in the obligately autogenous mosquito *Toxorhynchites amboinensis.*

MATERIALS AND METHODS

Insects

Mosquitoes used in the study were reared at 26°C, under a 12 h:12 h light:dark photoperiod and 70% relative humidity. The University of Georgia (UGAL) strain of *Aedes aegypti* (Linnaeus 1762) was established from field-captured material that was collected near Athens, GA, USA (Foster and Lea, 1975). The G3 strain of *Anopheles gambiae* Giles 1902 was obtained from the Centers for Disease Control and Prevention (CDC) in Atlanta in 2004, while the CDC MR4/BEI strain of *Culex quinquefasciatus* Say 1823 was obtained in 2011. *Aedes atropalpus* (Coquillett 1902) was obtained from the University of Arizona in 2006, *Toxorhynchites amboinensis* (Doleschall 1857) was obtained from Mercer County Mosquito Control (West Trenton, NJ, USA) in 2014, and *Culex pipiens molestus* Forskal was obtained from the University of California, Riverside, in 2015. Henceforth in the manuscript we refer to *Cx. pipiens molestus* as *Cx. pipiens*. Larvae of each species were reared in pans at a density of ∼150 larvae per liter of deionized water and fed daily until pupation. *Aedes aegypti* and *Cx. quinquefasciatus* were maintained on a larval diet consisting of ground rat chow pellets (LabDiet 5001), lactalbumin (Sigma-Aldrich) and torula yeast extract (Bio-Serve) mixed in a ratio of 1:1:1 by volume, referred to as rat chow mix. *Anopheles gambiae*, *Ae. atropalpus* and *Cx. pipiens molestus* larvae were maintained on a diet of pulverized TetraMin tropical flakes (Tetra). *Toxorhynchites amboinensis* larvae are predacious and were reared by feeding them *Ae. aegypti* larvae (Coon et al., 2020). Adult mosquitoes were provided water and 10% sucrose (w/v) in water *ad libitum*. For each anautogenous species, adult females produced eggs by feeding them defibrinated rabbit blood (Hemostat Laboratories) using a membrane feeder 3–5 days post-eclosion (Harrison et al., 2021). All procedures were approved under Animal Use Protocol A2018 02-002-A9, which was administered by The University of Georgia Institutional Animal Care and Use Committee (IACUC).

Reagents

Aedes aegypti ILP3 was produced by synthesizing the A and B chains using standard Fmoc chemistry followed by formation of the correct interchain disulfide bonds as previously described (Brown et al., 2008). Recombinant OEH was produced in *Escherichia coli* as reported earlier (Gulia-Nuss et al., 2012; Vogel et al., 2015). High performance liquid chromatography (HPLC) was used to confirm the integrity of ILP3 and to purify OEH as reported earlier (Brown et al., 2008; Gulia-Nuss et al., 2012; Vogel et al., 2015) (Fig. S1). Stock solutions of 20E (Sigma-Aldrich) were solubilized in ethanol. *Escherichia coli* K12 was grown in Luria broth to an optical density of 1.0, which equals ∼1×10^6 cells μl^{-1}. Bacteria were then heat-killed as previously described followed by storage at −80°C until use (Castillo et al., 2011). Each reagent was diluted to working concentrations in *Aedes* saline (238.4 mmol l^{-1} NaCl, 4.69 mmol l^{-1} KCl, 1.89 mmol l^{-1} $CaCl_2$) that was injected in a 1 µl volume into the mesothorax of each treated female using a glass needle.

Hemocyte abundance assays in *Ae. aegypti*

Four-day-old adult females were blood fed to repletion followed 2 h later by decapitation and injection of ILP3 (20 pmol), OEH (20 pmol), 20E (1 nmol) or saline using a glass needle mounted on a micromanipulator as per previously developed methods (Brown et al., 2008; Vogel et al., 2015). Hemocytes were collected 24 h later (see below). Samples were also collected from: intact (non-decapitated) females that were blood fed (BF) on day 4 followed by collection of hemocytes 24 h later; intact, non-blood-fed (NBF) females on day 5; and intact and NBF females that were injected with ILP3 (20 pmol) or 3×10^4 heat-killed *E. coli* cells on day 4 followed by collection of hemocytes on day 5. Hemocytes were collected from individual adult females by perfusion. In brief, mosquitoes were chilled on ice for 5–10 min followed by slowly injecting 20 µl of SFX cell culture medium (HyClone) using a glass needle mounted on a micromanipulator into the dorsal mesothorax, which caused the intersegmental membrane of an abdominal segment to rupture. The resulting perfusate consisting of SFX medium and hemolymph formed a drop on the surface of a Petri dish, which was collected and transferred to a well of a Teflon-coated microscope slide that was subdivided into 10 individual wells (Polysciences). Slides were placed in a Petri dish containing a moistened piece of tissue for 45 min at room temperature, which resulted in hemocytes settling on the surface of the slide and most granulocytes (see below) binding to and spreading to the surface of the slide. A coverslip was then placed over the slide, which was examined using a Leica DMRXE epifluorescent microscope fitted with differential interference contrast (DIC) optics. The total number of hemocytes recovered per female was then counted. Hemocyte counts were generated from a minimum of 20 females per treatment, with treatment comparisons analyzed by ANOVA and a *post hoc* Tukey–Kramer honest significant difference (HSD) test.

Reverse transcriptase (RT)-quantitative polymerase chain reaction (qPCR) assays

Hemocytes were collected from 4-day-old *Ae. aegypti* NBF females (0 h) and females that were blood fed on day 4 followed by sample collection 24 h PBM. Hemocytes were collected from a total of 30 individuals per biological treatment and replicate. Total RNA was extracted using 200 µl of Trizol reagent (Ambion) and RNA concentration was determined on a Nanodrop Spectrophotometer. cDNA templates were then generated from 1 µg of total RNA using the iScript cDNA synthesis kit (Bio-Rad). Transcript abundance of the *Ae. aegypti* insulin receptor (IR) (AAEL002317), OEH receptor (OEHR) (AAEL001915) and ecdysone receptor (EcR) (AAEL009600) was then determined by quantitative PCR (qPCR). Briefly, the full-length *Ae. aegypti* insulin receptor (IR, AAEL002317) and full-length *Ae. aegypti* OEH receptor (OEHR, AAEL001915) (Brown et al., 2008; Vogel et al., 2015) were cloned into pCMV-prolink1, while a portion of the *Ae. aegypti* ecdysone receptor (EcR, AY345989.1) was cloned into pCR2.1-TOPO during the present study using two specific primers (forward 5′-AAG-CGAGGTTATGATGTTGCG-3′; reverse 5′-CAGCAGGTCCTCT-ATCGTGTCC-3′) that were designed using Primer Premier 6 and purchased (IDT). Each plasmid was propagated in *Escherichia coli*, isolated by miniprepping (Qiagen) and Sanger sequenced to confirm identity (Eurofins). The threshold cycle (C_T) values for serial dilutions of 10^2–10^7 plasmid copies were then used to generate a

standard curve followed by experimental qPCR assays using hemocyte cDNA as template and the following primer sets (IR: forward 5′-TAATTCCACCTCCACCGAAG-3′; reverse 5′-CCGTTGGTTCTACTGCCTGT-3′; OEHR: 5′-TGTGTCATGACGATCGCGAT-3′; reverse 5′-CGGAATAGATGACGGCGACA-3′; EcR: forward 5′-AAGCGAGGTTATGATGTTGCG-3′; reverse 5′-CAGCAGGTCCTCTATCGTGTCC-3′). Results from each biological replicate were then fitted to the standard curve which generated an estimate for copy number of each transcript per nanogram of total RNA that was isolated per hemocyte sample. Standard curves and experimental qPCR assays were performed using a Rotor-Gene Q and QuantiFast SYBR Green PCR Kit 4000 (Qiagen) with 1 mmol l^{-1} primers and 1 µl of DNA or cDNA per 10 µl reaction under the following conditions: initial denaturation at 95°C for 10 min, followed by 45 cycles with denaturation at 95°C for 10 s, annealing at 55°C for 15 s and extension at 72°C for 20 s. Melting curve analyses were also performed to ensure that amplified products were specific for the gene of interest. Three independently acquired biological replicates were collected per treatment with each sample internally replicated four times. Copy number of each receptor per microgram of total RNA was compared between the 0 and 24 h PBM treatments by Student's *t*-test after confirming equal variances by Welch's test.

Ethynyl-2′-deoxyuridine labeling

Ethynyl-2′-deoxyuridine (EdU) incorporation into hemocytes was assessed by providing day 3 females 20% sucrose (w/v) containing 5 mmol l^{-1} EdU for 2 h (Sigma-Aldrich) (Valzania et al., 2019). Hemocytes were then collected 24 h post-treatment by perfusion and transferred to individual wells of Teflon-coated slides as described above. Most of the medium was then removed from the well, followed by the addition of 4% paraformaldehyde in phosphate buffered saline (PBS) for 20 min at room temperature (RT). After removing the fixative and washing two times with PBS, cells were permeabilized with 0.3% Triton X100 in PBS (PBT) for 1 h followed by visualizing the EdU labeled cells using the Click-iT® EdU Alexa Fluor 488 Imaging Kit (C10337, Thermo Fisher Scientific). The number of EdU-labeled hemocytes were then counted by visualizing the EdU signal using a 490 excitation/513 emission filter on the Leica DMRXE epifluorescent microscope fitted with a Leica camera and image acquisition software. Hemocytes from a minimum of 20 females per treatment were examined followed by comparison of treatments as described above for the total number of hemocytes recovered per female.

Immunoblotting and immunocytochemistry

Immunoblotting assays were conducted using abdominal pelts that consisted of fat body and epidermis with the ovaries and gut removed (Valzania et al., 2019). Pelts were collected from BF females at 6 h PBM and age-matched NBF females by dissection in PBS in PRO-PREP extraction solution (17081 Intron Biotechnology) with 1× protease and phosphatase inhibitors (Thermo Fisher Scientific). Protein concentration for each sample was determined using Coomassie Plus Protein reagent (Thermo Fisher Scientific). Samples were resuspended in Laemmli buffer with mercaptoethanol (10 µmol l^{-1}), boiled for 5 min and electrophoresed (75 µg per lane) on 4–20% Trish-HCl gels (Bio-Rad) followed by transfer to polyvinyl difluoride (PVDF; Thermo Fisher Scientific). After blocking in 5% nonfat dry milk in PBT, blots were probed overnight with primary antibodies to phosphorylated (p-) AKT (Thr^{342}) (1:1000; p104-342; PhosphoSolutions), p-ERK (1:1000; 4370S; Cell Signaling Technology) or actin (1:2000; A2103; Sigma-Aldrich) that was used as a loading control. Blots were then washed and probed with a peroxidase-conjugated goat anti-rabbit secondary antibody (1:5000; Jackson Labs) for 2 h, followed by visualization using a chemiluminescent substrate (Clarity; Bio-Rad) and a Syngene imaging system. Hemocytes were collected from NBF females, NBF females 24 h after injection with ILP3 and decapitation, BF females 24 h PBM, or BF females 24 h PBM after injection of ILP3 and decapitation as described above. Cells were fixed, permeabilized and rinsed with PBT followed by incubation in 5% goat serum and 0.3% Triton X100 in PBS (GS-PBT) for 1 h and addition of anti-p-AKT (1:100) or anti-p-ERK (1:100). After incubating with each primary antibody overnight at 4°C, hemocytes were washed in PBT and incubated with a goat-anti-rabbit Alexa-Fluor 488 or 568 secondary antibody (1:1000; Thermo Fisher Scientific) in GS-PBT at room temperature for 2 h. After washing, cells were cover slip mounted in 80% glycerol containing 4′,6-diamidino-2-phenylindole (DAPI; 1 µg ml^{-1}) and examined using epifluorescent microscopy as described above. Relative abundance of p-AKT and p-ERK per hemocyte was estimated by measuring pixel intensity using ImageJ software (National Institutes of Health, Bethesda, MD, USA), which calculates pixel intensity in arbitrary units. For each treatment, pixel intensities were measured in a minimum of 140 cells from four females using captured images that were acquired under identical exposure and gain conditions.

Transcriptome analyses

Hemocyte samples were prepared by collecting cells as described from 100 age-matched NBF females, 24 h PBM females and 24 h PBM females that were injected with ILP3 and decapitated. We also collected pelts containing fat body as described above from 30 age-matched NBF females, BF females 24 h PBM and BF females 24 h PBM that were injected with ILP3, OEH, 20E or *E. coli* and decapitated. For NBF and 24 h PBM females, we also collected whole guts from 30 age-matched females. We visually inspected hemocyte samples from each female and discarded samples where fat body cells were visible before pooling in order to reduce the risk of fat body contamination. Total hemocytes after pooling were pelleted by centrifuging 4 min at 500 ***g***, where the supernatant was removed and replaced with lysis buffer (Qiagen). Pelt and gut samples were placed directly in lysis buffer after dissection from females in physiological saline. Three independent sequencing libraries were prepared for each treatment by isolating total RNA from hemocytes, guts or pelts using the RNeasy Mini kit (Qiagen) followed by quantification and quality checking using Agilent 2100 Bioanalyzer. TruSeq mRNA (Illumina) library construction and 75 bp paired-end sequencing over three NextSeq High Output flow cells were then performed by the Genomics and Bioinformatics Core at the University of Georgia. cDNA for each sample was indexed with a unique adaptor. Each library was normalized by equimolar multiplexing. Pre-processing of raw reads included seqClean adaptor, uniVec database filtering and poly-A tail trimming, and quality trimming using the FASTX-Toolkit (http://hannonlab.cshl.edu/fastx_toolkit/) (Pearson et al., 1997) and quality was assessed using FastQC (http://www.bioinformatics.babraham. ac.uk/projects/fastqc). Processed reads were mapped to the official *Ae. aegypti* gene set (AaegL5.1) using the Burrows–Wheeler Aligner (BWA v.0.7.8) (Li and Durbin, 2010). Fragments per kilobase per million (FPKM) values were calculated in Cufflinks v.2.2.0 (Trapnell et al., 2010). DESeq v1.12.1 was used to generate normalized read counts and differential expression calls for each treatment (adjusted $P<0.01$) (Anders and Huber, 2010). The BioProject ID for the SRA files is

Journal of Experimental Biology (2022) 225, jeb243460. doi:10.1242/jeb.243460

PRJNA752401 and the BioSample accession numbers are SRX11658639–SRX11658719.

Hemocyte abundance assays in other mosquito species

Hemocyte abundance was measured in *Cx. quinquefasciatus* and *An. gambiae* females that were blood fed, injected with *Ae. aegypti* ILP3, *Ae. aegypti* OEH, 20E or saline and decapitated as described above for *Ae. aegypti*. Hemocytes were then collected 24 h post-treatment by perfusion with 24 h PBM non-decapitated females and age-matched NBF females serving as controls. Hemocytes were counted in the autogenous mosquito *T. amboinensis* within 24 h of eclosion, 3 days post-eclosion (after yolk was deposited in eggs), after oviposition of the first clutch of eggs, and 24 h after injecting 200 pmol of *Ae. aegypti* ILP3 into a decapitated <24 h post-eclosion female. The larger amount of ILP3 was injected because this species is ∼10× larger than *Ae. aegypti*. We measured hemocyte abundance in the facultatively autogenous mosquitoes *Ae. atropalpus* and *Cx. pipiens molestus* 3 h after adult emergence, 3 days post-emergence, and 24 h after injecting 20 pmol of ILP3 into a decapitated <3 h post-eclosion female. Three days after laying an autogenous first clutch, *Ae. atropalpus* females were blood fed followed by injection of ILP3 and decapitation and collection of hemocytes 24 h later as described above. Hemocytes from non-decapitated females that were collected 24 h PBM served as the positive control. A minimum of 20 females were analyzed per treatment followed by data analysis as described above for total hemocytes recovered from *Ae. aegypti*.

Data analysis and figure assembly

Data were statistically analyzed using JMP pro 15 (SAS). Graphs were generated using GraphPad Prism software and ggplot2, while composite figures were assembled using Adobe Photoshop and Adobe Illustrator.

RESULTS

ILP3 stimulates hemocytes to proliferate in *Ae. aegypti* but OEH and 20E do not

Decapitating *Ae. aegypti* females by 2 h PBM ablates the endogenous source of the ILPs and OEH that activate primary follicles (Valzania et al., 2019). As a result, 20E biosynthesis by follicle cells, vitellogenesis by the fat body, and yolk deposition into oocytes is fully inhibited, whereas injection of 20 pmol of ILP3, 20 pmol of OEH or 1 nmol of 20E into decapitated females rescues egg formation (Brown et al., 1998, 2008; Wen et al., 2010; Vogel et al., 2015; Valzania et al., 2019). Although prior results showed that hemocytes express the insulin receptor (IR) (Castillo et al., 2011), we did not examine whether hemocytes also express the ecdysone receptor (EcR) or the OEH receptor (OEHR), which at the time had not been identified (Vogel et al., 2015). We therefore began this study by measuring transcript abundance for the IR, OEHR and EcR in hemocytes collected from NBF and 24 h PBM females. Results showed that blood feeding increased transcript abundance of each, but IR and EcR copy numbers were higher than for the OEHR (Fig. 1A). As each receptor was detected in hemocytes at the RNA level, we next asked whether each ligand stimulated circulating hemocytes to increase in abundance by comparing intact, BF females at 24 h PBM (positive control) with age-matched NBF females (negative control) and decapitated, BF females 24 h after injection of ILP3 (20 pmol), OEH (20 pmol), 20E (1 nmol) or saline. Hemocyte abundance equivalently increased in ILP3-treated and intact (non-decapitated) BF females, whereas OEH, 20E or saline had no stimulatory effect (Fig. 1B). ILP3 also

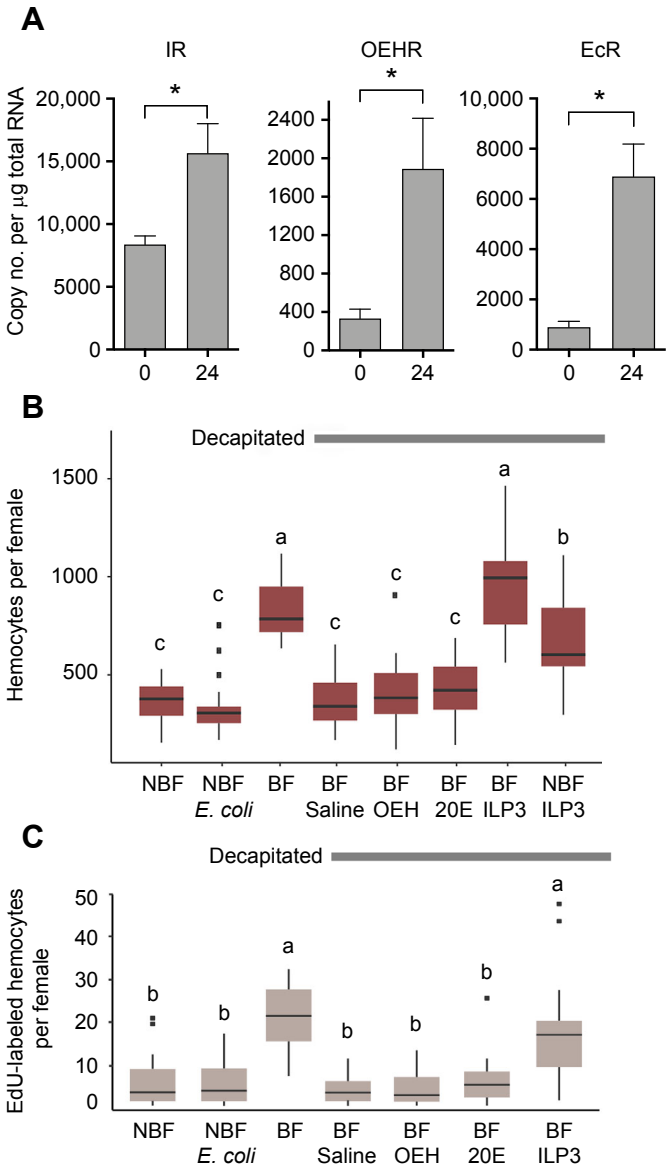

Fig. 1. *Aedes aegypti* hemocytes express the insulin receptor (IR), ovary ecdysteroidogenic hormone receptor (OEHR) and ecdysone receptor (EcR), but only insulin-like peptide 3 (ILP3) stimulates cells to increase in abundance. (A) Transcript abundance of the IR, OEHR and EcR in hemocytes before a female blood feeds (0 h) and 24 h post-blood meal (PBM) as determined by absolute qPCR. For each gene, an asterisk above the bars indicates transcript abundance significantly differed (unpaired *t*-test with Welch's correction; $P<0.05$). (B) Boxplots of hemocyte counts from non-blood-fed (NBF) mosquitoes, NBF females injected with heat-treated *E. coli*, intact blood-fed (BF) females at 24 h PBM, decapitated BF females at 24 h PBM that were injected with saline, OEH, 20E or ILP3, and decapitated NBF females at 24 h post-injection that were injected with ILP3. Different letters above a given treatment indicate means that significantly differ ($F_{7,159}=42.1$, $P<0.001$). (C) Boxplots showing the number of hemocytes that were EdU labeled for all of the same treatments as shown in B, except that no NBF females injected with ILP3 were examined. Different letters indicate means that significantly differ ($F_{6,104}=15.3$, $P<0.001$).

stimulated hemocytes to increase in decapitated, NBF females relative to intact NBF females (negative control) but values were lower when compared with the positive control (Fig. 1B).

Aedes aegypti and other mosquitoes produce three major types of hemocytes that are distinguished by morphological, functional and

Journal of Experimental Biology (2022) 225, jeb243460. doi:10.1242/jeb.243460

molecular markers (Castillo et al., 2006; Hillyer and Strand, 2014; Bryant and Michel, 2016; Severo et al., 2018; Raddi et al., 2020; Kwon et al., 2021). Granulocytes, which account for more than 90% of the hemocytes in circulation in *Ae. aegypti* and *An. gambiae*, are adhesive, binding to a variety of foreign surfaces, and phagocytic. Molecular markers further distinguish granulocyte subpopulations, including one that expresses mitotic markers (Raddi et al., 2020). Oenocytoids comprise 3–5% of the hemocytes in circulation, are weakly adhesive, and express several markers with functions in differentiation and functional activities including phenoloxidases (PPOs) that catalyze the formation of melanin (Severo et al., 2018; Raddi et al., 2020; Kwon et al., 2021). Prohemocytes are non-adhesive and comparatively rare in circulation, but express markers in *An. gambiae* that suggest they may be progenitor cells that differentiate into granulocytes (Raddi et al., 2020). As in *An. gambiae*, granulocytes from *Ae. aegypti* phagocytize bacteria such as *E. coli* (Castillo et al., 2006; Baton et al., 2009; Reynolds et al., 2020). We thus asked in this study whether injection of bacteria into the hemocoel of NBF adult females also increased the abundance of hemocytes in circulation 24 h post-challenge, but results showed it did not (Fig. 1B). We also fed *Ae. aegypti* females the thymidine analog EdU to determine whether the number of hemocytes that synthesized DNA increased in response to ILP3, OEH, 20E or *E. coli*. The number of EdU-labeled hemocytes 24 h post-treatment increased in ILP3-treated and intact, BF females (positive control) but were unchanged in saline, OEH, 20E or *E. coli* treated females relative to the NBF negative control (Fig. 1C). On the basis of morphological characters that distinguish the hemocyte types in *Ae. aegypti* (Castillo et al., 2006), all of the EdU-labeled hemocytes we observed across treatments were granulocytes.

ILP3 binds the IR in *Ae. aegypti* with high affinity (Wen et al., 2010), while RNAi knockdown of the IR in hemocytes inhibits proliferation, as noted earlier (Castillo et al., 2011). Because OEH and 20E had no effect on hemocyte proliferation, we focused on whether ILP3 activated insulin-insulin growth factor signaling (IIS) by monitoring the phosphorylation status of AKT and ERK, which are markers for activation of the phosphatidylinositol-3-kinase/protein kinase B (PI3K/AKT) and mitogen activated protein kinase (MAPK/ERK) branches (Teleman, 2010; Roy et al., 2007; Pakpour et al., 2012; Valzania et al., 2019). On immunoblots, the primary antibodies we used readily detected *Ae. aegypti* p-AKT and p-ERK in pelt extracts, while also showing that p-AKT and p-ERK were much higher in pelts from BF females than NBF females (Fig. 2). Therefore, we used these antibodies in immunocytochemical assays, which showed that p-AKT and p-ERK were also significantly higher in hemocytes from BF females than NBF females (Fig. 3A,B). Because only ILP3 stimulated hemocyte proliferation, we also assessed whether ILP3 injection into intact NBF and BF females that were decapitated also stimulated p-AKT and p-ERK to increase in hemocytes. Outcomes showed that phosphorylation of both markers increased in response to ILP3 when compared with hemocytes from control females (Fig. 3C,D). The preceding results thus indicated that ILP3 stimulates *Ae. aegypti* hemocytes to proliferate but OEH and 20E do not. ILP3-induced proliferation was further associated with increased signaling through both the PI3K/AKT and MAPK/ERK branches of the IIS pathway.

Hemocyte transcriptome samples were minimally contaminated by fat body while expressing multiple blood cell markers

We next conducted an RNA-Seq analysis of hemocytes from NBF females, 24 h PBM females and decapitated 24 h PBM females

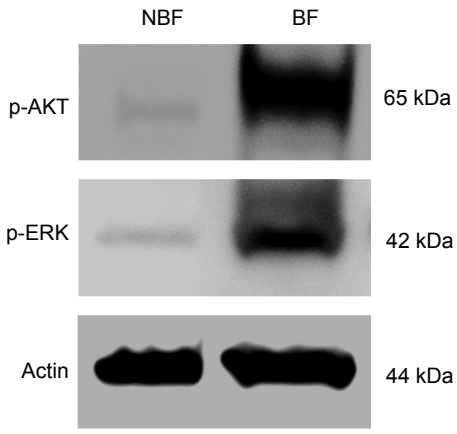

Fig. 2. Immunoblotting indicates that p-AKT and p-ERK levels increase in pelts from BF females when compared with NBF females. Samples were collected 6 h PBM from BF females and age-matched NBF females and were probed with antibodies to p-AKT, p-ERK or actin, which served as a loading control. Molecular masses of each protein are indicated to the right of each blot.

injected with ILP3. Sequencing libraries from abdominal pelts containing fat body and whole guts were also prepared for use as controls for selected comparisons with hemocytes. In total, we sequenced 33 libraries that, after quality filtering, yielded 368 million paired-end reads. We further used *Ae. aegypti* LVP_AGWG_TRANSCRIPTS_AaegL5.1.fa as the official gene set for *Ae. aegypti* from VectorBase (https://vectorbase.org/vectorbase/app/record/dataset/DS_cc8d875d2e). This gene set consists of 34,403 transcripts. Mapping our quality-filtered reads to this gene set identified a total of 18,128, 16,867 and 15,043 transcripts in our hemocyte, pelt and gut libraries, respectively, that had an FPKM ≥1. Pelts and guts were easily collected for RNA-Seq library construction, whereas hemocytes were more difficult owing to the relatively small number of cells that can be collected per female and the potential for contamination from fat body cells that can be dislodged during perfusion. We attempted to minimize the latter by inspecting each sample and discarding those containing visible fat body cells before pooling hemocytes for library construction. We further assessed the quality of our hemocyte libraries by determining FPKM values for *vitellogenins*, which are fat body marker genes that, as earlier noted, are also strongly upregulated in response to blood feeding (Roy et al., 2007; Valzania et al., 2019; Wang et al., 2017). FPKM values for the three *vitellogenin-A1* isoforms (AAEL006126-RA, AAEL006138-RA, AAEL010434-RA) averaged 2580 FPKM in the pelt transcriptomes from BF females but only 1.15 FPKM in our hemocyte libraries. We also examined our hemocyte libraries for expression of the 548 genes identified by Raddi et al. (2020) as hemocyte markers. Results indicated that 65.5% of these genes had FPKM values ≥10, while 91% had FPKM values ≥2, which further supported our hemocyte libraries consisting primarily of blood cells (Table S1).

Genes with functions in the IIS pathway and mitosis are expressed in hemocytes but are not differentially expressed in response to blood feeding or injection of ILP3

Given evidence that our hemocyte libraries were minimally contaminated, we next focused on genes with functions in the IIS pathway and proliferation. The IIS pathway is primarily regulated post-translationally via differential phosphorylation of downstream proteins after ILP binding to the IR (Nassel et al., 2015; Strand et al., 2016; Valzania et al., 2019). Thus, our preceding results showing

Journal of Experimental Biology (2022) 225, jeb243460. doi:10.1242/jeb.243460

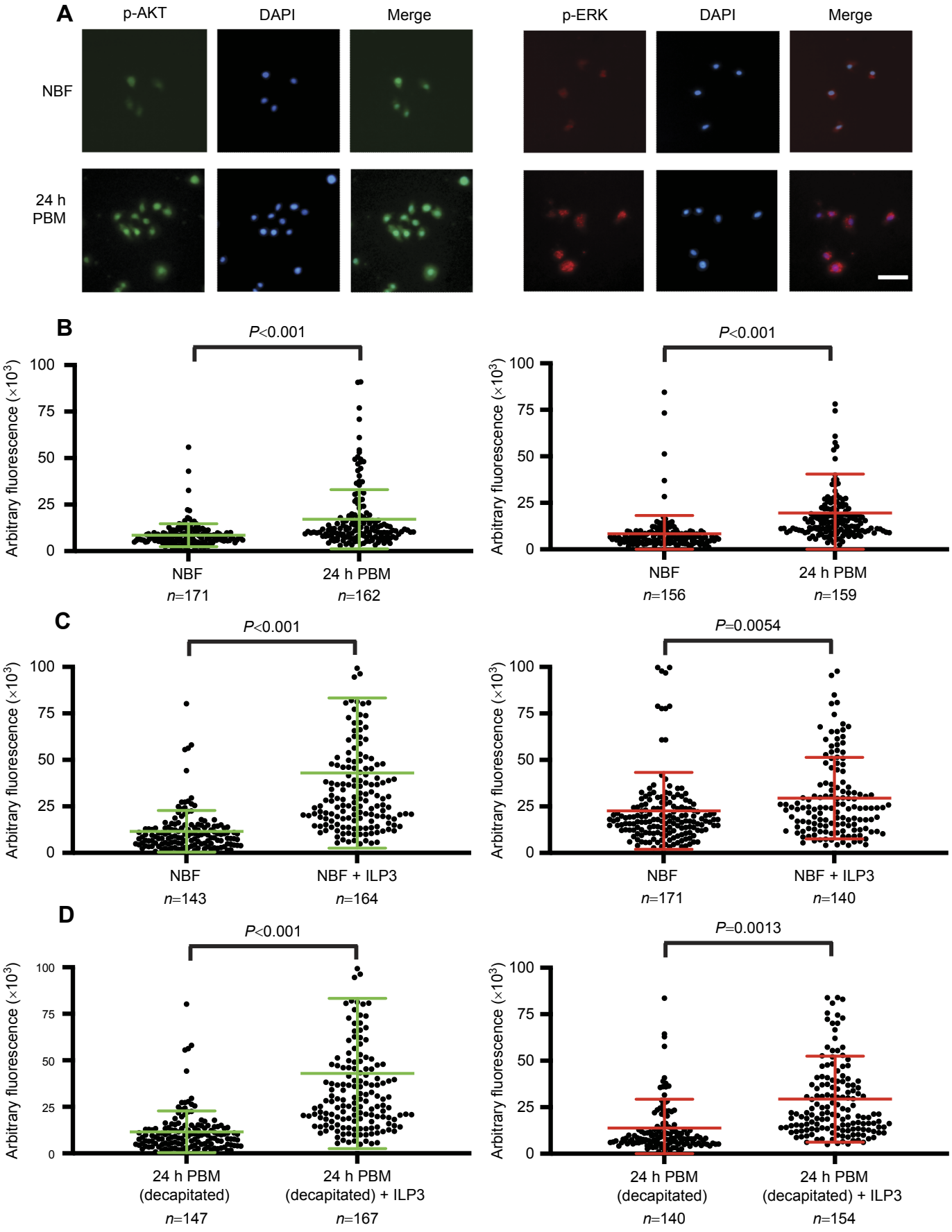

Fig. 3. See next page for legend.

Journal of Experimental Biology (2022) 225, jeb243460. doi:10.1242/jeb.243460

Fig. 3. p-AKT and p-ERK levels increase in granulocytes after blood feeding or injection of ILP3 into decapitated females. (A) Epifluorescent microscopy images of granulocytes from NBF and 24 h PBM females after labeling with anti-pAKT (left) or anti-pERK (right), and DAPI that stains DNA in nuclei (blue). Merged images show cells labeled with each antibody plus DAPI. Scale bar in the lower right panel is 30 µm. (B) Quantification of p-AKT (left) or p-ERK (right) in granulocytes from NBF females and 24 h PBM females in arbitrary pixel intensity units. The number of cells from four females that were measured is indicated below each treatment. An unpaired *t*-test with Welch's correction indicated pixel intensity units were significantly higher in granulocytes from 24 h PBM females than NBF females (unpaired *t*-test with Welch's correction). (C) Quantification of p-AKT (left) and p-ERK labeling in granulocytes from age-matched NBF females and decapitated NBF females 24 h after injection of ILP3 in arbitrary pixel intensity units. The number of cells measured and significance values are defined as in B. (D) Quantification of p-AKT (left) and p-ERK (right) labeling in granulocytes from decapitated BF females injected with saline at 24 h PBM females and decapitated BF females injected with ILP3 at 24 h PBM in arbitrary pixel intensity units. The number of cells measured and significance values are defined as in B.

that blood feeding and ILP3 both increase p-AKT and p-ERK in hemocytes were fully consistent with ILP3 activating the IIS pathway by inducing the phosphorylation of key pathway components (Fig. 3). In contrast, we detected no differences in transcription of *akt*, *erk* or ribosomal protein S6 (=*S6K*) in either hemocytes or the fat body (=pelts) from NBF-, BF- and ILP3-injected females (Table 1). Reciprocally, genes in the ecdysone signaling pathway such as *E74* and *E75* are known to be transcriptionally upregulated by 20E in the fat body (Roy et al., 2007; Wang et al., 2017, 2021). Consistent with expectation, FPKM values for *E74* and *E75* were significantly higher in pelts from intact BF females at 24 h PBM and BF females at 24 h PBM that were injected with 20E and decapitated (Table 1). Injection of ILP3 and OEH, which stimulate the ovaries to produce 20E (Brown et al., 2008; Vogel et al., 2015), also upregulated *E74* and *E75* in BF females that were decapitated (Table 1). However, no differences in *E74* and *E75* transcription were detected among treatments in hemocytes (Table 1). Among the hemocyte markers identified by Raddi et al. (2020) were several cyclins and a threonine-kinase that produce essential proteins for mitosis. FPKM values for each of these genes were significantly higher in hemocytes when compared with the gut, but none had FPKM values that significantly differed between NBF females, BF females, and BF females that were injected with ILP3 and decapitated (Table 2). Altogether, these findings supported that ILP3 stimulates proliferation by activating the IIS pathway in hemocytes, but does not transcriptionally upregulate downstream pathway genes such as *akt*, *erk* and *s6 kinase*, or previously identified mitotic marker genes.

Few genes are differentially expressed in hemocytes in response to blood feeding or ILP3

The final goal of our RNA-Seq analysis was to identify genes that were significantly differentially expressed or gene sets that were differentially overrepresented in hemocytes from NBF females, BF females at 24 h PBM, or BF females at 24 h PBM that had been injected with ILP3 and decapitated. Given evidence that ILP3 stimulates hemocytes to proliferate, we also were especially interested in whether any genes with known immune functions were upregulated. Toward these goals, we first determined that 5546 genes had FPKM values ≥10 in at least one of our hemocyte libraries, indicating that 17% of the 34,403 genes in the reference gene set (AaegL5.1.fa) were at least moderately expressed (Table S2). Among these genes, 81.8% (4536 genes) had comparable FPKMs among our three treatments, while only 158, 108 and 262 were preferentially detected in hemocytes from NBF females, BF females or BF females injected with ILP3, respectively (Fig. 4A; Table S2). However, only four of the 262 genes that were preferentially detected in hemocytes from the ILP3 treatment (two cuticle proteins, a fatty acid hydroxylase and an N-oxygenase) were significantly differentially expressed when compared with hemocytes from NBF females. A gene ontology (GO) enrichment analysis further identified 20 overrepresented terms among the 262 genes from the ILP3 treatment (Table S3). More than half of these GO terms had functions in lipid metabolism, which the IIS pathway is well known to affect in insects (summarized by Nassel et al., 2015), while none had known immune functions.

Expanding our analysis to all transcripts detected in hemocytes, regardless of FPKM, we identified a total of 91 genes that were significantly differentially expressed among our three treatments (Table S4). As shown in Fig. 3B, 67 of these genes (0.2% of the gene set) were differentially expressed between hemocytes from BF females injected with ILP3 and NBF females, 36 were differentially expressed between hemocytes from BF females injected with ILP3 and BF females, and 13 were differentially expressed between hemocytes from BF females injected with ILP3 and hemocytes from

Table 1. Average FPKM values for *Aedes aegypti* genes in the insulin-insulin growth factor (IIS) and ecdysone signaling (ES) pathways

Ae. aegypti gene	NCBI gene description	NBF hemocyte	BF hemocyte	ILP3 hemocyte	NBF pelt	BF pelt	ILP3 pelt	OEH pelt	20E pelt	*E. coli* pelt
AAEL003163-RB	Protein fork head (IIS)	0.49	0.54	0.20	0.27	0.00	0.01	0.00	0.01	0.00
AAEL008823-RA	RAC serine/threonine-protein kinase (=AKT) (IIS)	2.20	1.87	1.03	5.33	1.59	2.30	4.11	1.59	5.98
AAEL013939-RB	Mitogen-activated protein kinase (=ERK) (IIS)	0.88	1.17	0.49	1.00	0.38	0.26	0.30	0.22	0.61
AAEL018120-RA	Ribosomal protein S6 kinase beta-2 (=S6K) (IIS)	1.60	1.32	0.91	2.01	0.24	0.33	0.61	0.23	3.14
AAEL004572-RC	Mushroom body large-type Kenyon cell-specific protein 1 (=E93) (ES)	0.06	0.17	0.11	1.19	0.82	1.05	1.27	0.87	1.17
AAEL007397-RA	Ecdysone-inducible protein E75 (ES)	5.60	4.78	3.28	1.98	7.48*	8.33*	6.18*	4.47*	0.72
AAEL019431-RB	Ecdysone receptor (ES)	1.49	1.95	1.05	2.73	3.18	2.57	4.48	2.45	2.27
AAEL023348-RA	Ecdysone-induced protein 74EF (=E74) (ES)	3.90	4.99	4.72	1.93	14.02*	6.22*	6.93*	7.84*	1.53

IIS, insulin-insulin growth signaling pathway; ES, ecdysone signaling pathway. FPKM values are the average from three biological replicates for the following samples: hemocytes and pelts (=fat body) from NBF females, BF females 24 h PBM, and decapitated BF females injected with ILP3 at 24 h PBM. Also presented are FPKM values for pelts from decapitated BF females injected with OEH, 20E or heat-killed *E. coli*. Asterisks (*) indicate FPKM values for E74 or E75 in pelts from BF females at 24 h PBM, or BF females at 24 h PBM that were injected with ILP3, OEH or 20E differed when compared with pelts from age-matched NBF females (unpaired *t*-test, $P \leq 0.05$).

Journal of Experimental Biology (2022) 225, jeb243460. doi:10.1242/jeb.243460

Table 2. FPKM values for *Ae. aegypti* cyclins and threonine kinases implicated in regulating mitosis

Ae. aegypti gene	NCBI gene description	NBF hemocyte	BF hemocyte	ILP3 hemocyte	NBF gut	BF gut
AAEL000672-RA	G2/mitotic-specific cyclin-A	26.37*	26.84**	25.38**	5.47	4.93
AAEL004492-RA	Cyclin-dependent kinases regulatory subunit	28.92*	23.82**	32.52**	0.88	1.76
AAEL004865-RA	Cyclin G	144.59	143.34**	136.18**	128.62	216.24
AAEL010094-RA	G2/mitotic-specific cyclin-B	40.89*	33.96**	31.26**	3.37	2.73
AAEL006712-RA	Aurora kinase B	15.11*	13.81**	13.67**	1.00	0.82
AAEL006977-RA	Serine/threonine-protein phosphatase PP2A 65 kDa regulatory subunit	82.18*	85.21	83.49**	67.25	48.09
AAEL009880-RA	Aurora kinase C	10.44*	10.82**	8.94**	0.47	0.50
AAEL015216-RA	Nucleosomal histone kinase 1	1.78	1.86	1.94**	0.99	0.57

FPKM values are the average from three biological replicates for the following samples: hemocytes and whole gut from NBF females, hemocytes and whole gut from BF females 24 h post-blood meal, and hemocytes from BF females injected with ILP3 and decapitated at 24 h post-blood meal. An asterisk (*) indicates the FPKM value for the gene in hemocytes from NBF females significantly differed from the FPKM value in whole gut from NBF females (unpaired *t*-test, $P<0.05$). A double asterisk (**) indicates the FPKM value for the gene in hemocytes from intact BF females at 24 h PBM or decapitated BF females at 24 h PBM that were ILP3 injected significantly differed from the FPKM value in whole gut from intact BF females at 24 h PBM (unpaired *t*-test, $P<0.05$).

both BF and NBF females (Fig. 4B). Inspection of this gene list indicated most code for enzymes or genes with uncharacterized functions while only three are known immune genes (Table S3). One of these, peptidoglycan-recognition protein SC2 (AAEL017056), had an average FPKM of 2580 in hemocytes from decapitated BF females injected with ILP3, which was 2.6-fold higher than in hemocytes from NBF mosquitoes. The other two were C-type lectins (AAEL011404-RA and AAEL011407-RA) that were 9.3- and 7.1-fold higher in hemocytes from decapitated BF females injected with ILP3 versus NBF females, but were not differentially expressed when intact BF females were compared with NBF females, which suggested their upregulation in the ILP3 treatment was likely due to damaging the exoskeleton by decapitation, and ILP3 injection (Table S3). Given these findings, we further examined transcript levels for 119 other genes in the *Ae. aegypti* genome with known immune functions including multiple recognition and signaling factors, components of the phenoloxidase cascade, and several effector molecules that included antimicrobial peptides (AMPs) and complement-like proteins (Blandin and Levashina, 2007; Lemaitre and Hoffmann, 2007; Hillyer and Strand, 2014). Each of these genes was similarly expressed in hemocytes from NBF females, intact 24 h PBM females and decapitated 24 h PBM females injected with ILP3 (Table S5), which was further illustrated by presenting each gene and treatment in a heat map (Fig. 4C). We thus concluded that relatively few genes with known immune functions were significantly upregulated in association with ILP3-induced proliferation.

ILP3 increases the abundance of circulating hemocytes in other anautogenous and facultatively autogenous species but not in an obligately autogenous species

All sequenced mosquito species in genomic databases have multiple ILP genes, a single copy OEH gene, and a single copy IR, OEHR and EcR (Vogel et al., 2013; Strand et al., 2016). Consistent with this conservation, previous functional assays also indicate *Ae. aegypti* ILP3 and OEH stimulate egg formation in other *Aedes* and *Anopheles* spp. at similar concentrations as *Ae. aegypti* itself (Strand et al., 2016; Gulia-Nuss et al., 2012; Nuss et al., 2018). Therefore, we used ILP3 and OEH from *Ae. aegypti* plus 20E to assess whether any of these hormones stimulated hemocytes in circulation to increase in abundance in two other anautogenous species: *Cx. quinquefasciatus*, which, like *Ae. aegypti*, is in the subfamily Culicinae, and *An. gambiae*, which is in the Anophilinae. For both, we compared intact BF females at 24 h PBM (positive control) and age-matched NBF females (negative control) to decapitated BF females 24 h PBM after injection of ILP3, OEH, 20E or saline. Results indicated that ILP3 stimulated hemocytes to increase to similar levels as the positive control while OEH and 20E did not (Fig. 5).

Facultatively autogenous mosquitoes produce a first clutch of eggs without blood feeding but must blood feed to produce additional clutches (Rioux et al., 1975; O'Meara, 1985; Attardo et al., 2005; Provost-Javier et al., 2010). *Aedes atropalpus* is a facultatively autogenous species that produces a first clutch 3–4 days post-emergence in response to blood-meal-independent release of ILPs and OEH followed by blood-meal-dependent release of ILPs and OEH if a female produces a second clutch (Gulia-Nuss et al., 2012). Time course assays showed that during the first autogenous egg maturation cycle, hemocyte abundance in *Ae. atropalpus* declined from 3 to 72 h post-emergence as well as after oviposition on day 4 (Fig. 5). Injection of ILP3 at 3 h post-emergence followed by assessment 24 h later resulted in hemocyte abundances that were lower than at 3 h post-emergence but higher than at 72 h or after oviposition (Fig. 5). We then blood fed females at 6 days and compared intact BF females 24 h PBM (positive control) with decapitated BF females at 24 h PBM that were injected with ILP3. Results showed that hemocyte abundance was slightly higher in intact 24 h PBM females, while ILP3 injection resulted in hemocyte abundance increasing to similar levels as observed in newly emerged (3 h) females (Fig. 5). *Culex pipiens molestus* is also a facultatively autogenous species that lays eggs 3–4 days post-emergence but will only sometimes consume a blood meal and lay a second clutch (Kassim et al., 2012; Gao et al., 2019). Hemocyte abundance declined in intact *Cx. pipiens* from 3 h post-emergence to oviposition on day 4, but injection of ILP3 into females that were decapitated at 3 h post-emergence stimulated hemocytes to increase (Fig. 5). A small number of females blood fed after laying a first clutch, which also resulted in hemocyte abundance increasing, but we were unable to inject ILP3 into decapitated BF females because too few individuals blood fed to generate a sample that could be compared with the other treatments. Lastly, we examined *T. amboinensis*, which is an obligately autogenous culicine (Donald et al., 2020; Coon et al., 2020). In this species, time course studies showed that hemocyte abundance was similar between newly emerged and 72 h post-emergence females, but was lower in 4- to 5-day-old females that had laid eggs (Fig. 5). Injection of ILP3 into 3 h post-emergence females that were decapitated followed by measuring hemocyte abundance 24 h later showed no stimulatory effect (Fig. 5).

Journal of Experimental Biology (2022) 225, jeb243460. doi:10.1242/jeb.243460

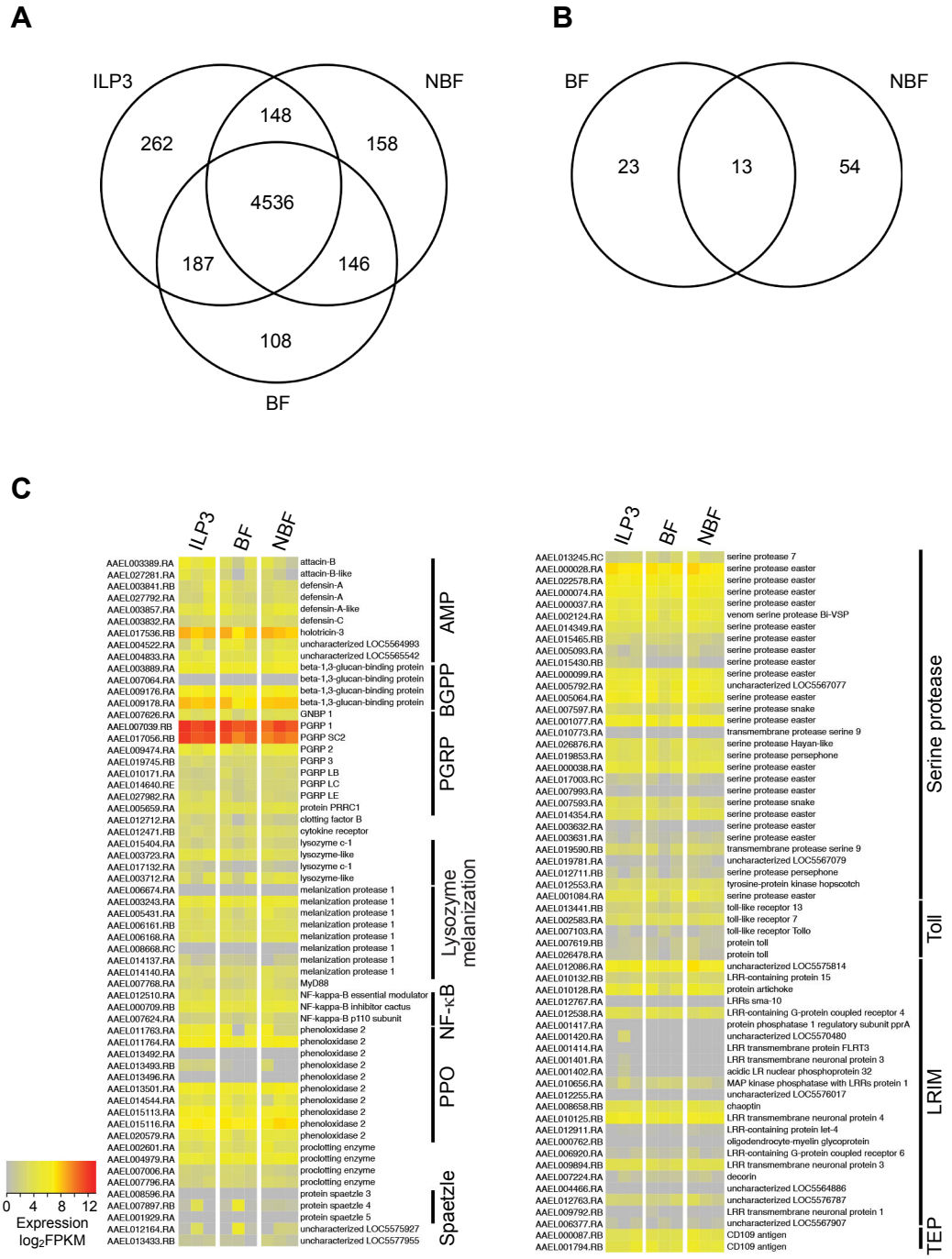

Fig. 4. RNAseq profiles for hemocytes collected from intact BF females at 24 h PBM (BF), decapitated BF females at 24 h PBM that were injected with ILP3 (ILP3), and age-matched NBF females (NBF). (A) Venn diagram showing the overlap of genes expressed with an average expression of >10 FPKM across three biological replicates for each treatment. (B) Venn diagram showing significantly differentially expressed genes in hemocytes from intact NBF females or intact BF females at 24 h PBM when compared to decapitated BF females at 24 h PBM that were injected with ILP3. (C) A heatmap showing high (red), low (yellow) and no (gray) gene expression in $\log_2$FPKM (fragments per kilobase of transcript per million mapped reads) in the three treatments. Each treatment derives from three independent biological samples that are presented in Table S3. Larger categories of immune genes are labeled above as: AMP, antimicrobial peptides; BGBP, β-1,3-glucan-binding protein; PGRP, peptidoglycan recognition protein; NF-κB, nuclear factor-κB; PPO, prophenoloxidase; TEP, thioester-containing protein; LRIM, Leucine-Rich repeat Immune protein.

DISCUSSION

The Culicidae is an ancient group in which the Anophilinae and Culicinae diverged approximately 200 million years ago (Bertone et al., 2008; Reidenbach et al., 2009). Virtually all anophilines and most culicines are anautogenous, which, combined with the basal position of the Anophilinae in the Culicidae overall, suggests mosquitoes evolved from a blood-feeding ancestor. Thereafter though, facultative autogeny has arisen several times in the Culicinae while three genera including *Toxorhynchites* are thought to consist entirely of obligately autogenous species (Rioux et al., 1975; O'Meara, 1985; Bradshaw et al., 2018). One factor thought to underlie why most mosquitoes remain

Journal of Experimental Biology (2022) 225, jeb243460. doi:10.1242/jeb.243460

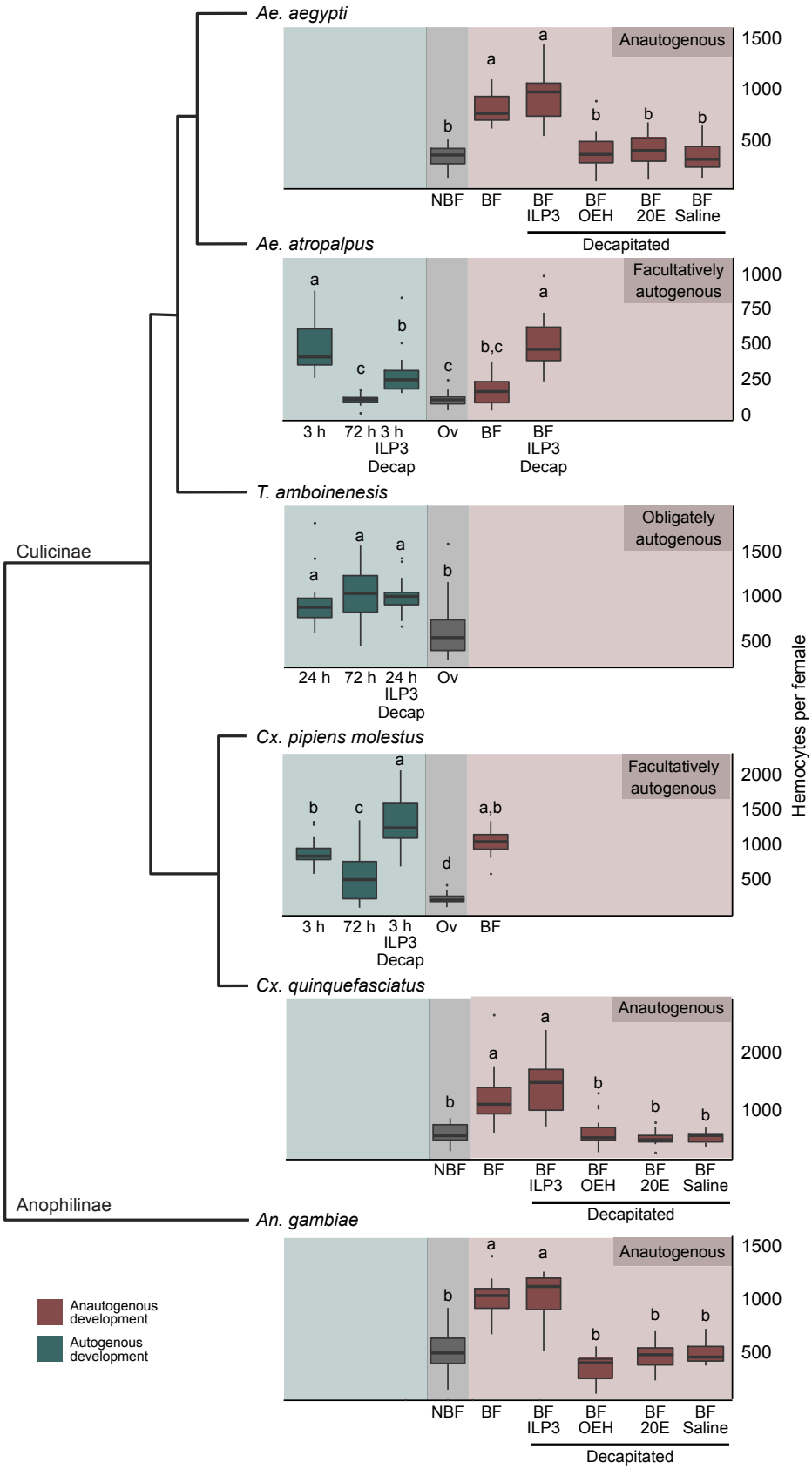

Fig. 5. ILP3 stimulates hemocyte abundance to increase in two anautogenous species (*Anopheles gambiae*, *Culex quinquefasciatus*) and two facultatively autogenous mosquitoes (*Aedes atropalpus*, *Culex pipiens molestus*), but does not do so in obligately autogenous *Toxorhynchites amboinensis*. The phylogenetic placement of each species in the Anophilinae and Culicinae is shown. For *Ae. aegypti*, the information from Fig. 1B is presented again to facilitate comparison. For *An. gambiae* and *Cx. quinquefasciatus*, box plots of hemocyte counts are shown from NBF mosquitoes, intact, BF females at 24 h PBM, decapitated BF females at 24 h PBM that were injected with ILP3, OEH, 20E or saline. Different letters indicate means that significantly differ in *An. gambiae* ($F_{3,79}$=56.8; P<0.001) or *Cx. quinquefasciatus* ($F_{3,79}$=27.5, P<0.001). For *Ae. atropalpus* and *Cx. pipiens* , box plots of hemocyte counts are shown from intact NBF females at 3 h post-emergence, intact NBF female at 72 h post-emergence, NBF female at 3 h injected with ILP3 and sampled 24 h later, intact NBF female at 96 h after ovipositing a first clutch (OV), BF female at 24 h PBM, and decapitated BF females at 24 h PBM that was injected with ILP3. Different letters indicate means that significantly differ in *Ae. atropalpus* ($F_{4,119}$=39.6, P<0.001) or *Cx. pipiens* ($F_{4,90}$=41.8, P<0.001). For *T. amboinensis,* box plots of hemocyte counts are shown from intact NBF females at 24 h post-emergence, intact NBF female at 72 h post-emergence, NBF female at 3 h injected with ILP3 and sampled 24 h later, intact NBF female at 96 h after ovipositing a first clutch (OV). Different letters above each plot indicate treatments that differed ($F_{3,79}$=8.8, P<0.001).

anautogenous is that adults emerge from an aquatic larval stage with insufficient nutrient reserves to produce eggs (Attardo et al., 2005). Most larval stage mosquitoes feed on plant-derived detritus that is often protein poor, whereas vertebrate blood by dry mass primarily consists of protein (Merritt et al., 1992; Yee et al., 2007; Harrison et al., 2021). However, life history shifts such as larval stage

Toxorhynchites spp. becoming predators and other strategies that increase nutrient reserves in larvae and newly emerged adults have likely contributed to the evolution of autogeny (Attardo et al., 2005; Bradshaw et al., 2018; Coon et al., 2020; Donald et al., 2020). Mortality risks from blood feeding via hosts or infection could also affect the favorability of anautogenous versus autogenous reproduction (Tsuji et al., 1990).

Transiently increasing hemocyte abundance after blood feeding potentially reduces infection risks as a form of anticipatory defense (Castillo et al., 2011; Bryant and Michel, 2016). Regulating anticipatory defense functions through the endocrine factors that control egg formation could also be less energetically costly than constitutively maintaining basal immunity at elevated levels (Upton et al., 2015). However, prior studies have largely lacked a comparative component to assess whether the increase in circulating hemocytes that occurs in species such as *Ae. aegypti* and *An. gambiae* is regulated by the same endocrine factors (Castillo et al., 2006, 2011; Bryant and Michel, 2014). Additionally unknown is whether circulating hemocytes also increase in abundance in facultatively autogenous mosquitoes that can still blood feed versus obligately autogenous species which would be expected to experience different infection risks given females never blood feed. Focusing first on *Ae. aegypti*, our results show that hemocytes express the IR, OEHR and EcR but only ILP3 stimulates proliferation. Our comparative results show that ILP3 also stimulates circulating hemocytes to increase in two other anautogenous species (*An. gambiae* and *Cx. quinquefasciatus*) and two facultatively autogenous species (*Ae. atropalpus* and *Cx. pipiens*), but not in *T. amboinensis*. Overall, these outcomes suggest hemocyte proliferation in association with blood feeding is a conserved, ILP-induced response in anautogenous mosquitoes but has been lost in at least one obligately autogenous species that no longer experiences potential infection risks associated with blood feeding. Other obligately autogenous species clearly need to be studied to determine whether they are similarly insensitive to ILP treatment, but this is also currently difficult because few obligately autogenous mosquitoes are in culture and available for study. Additional functional experiments will also be required to understand the mechanism(s) underlying why hemocytes in *T. amboinensis* do not respond to ILP stimulation.

Vertebrate ILPs are subdivided into: (1) insulin that primarily regulates metabolic functions and preferentially binds the IR, (2) insulin-like growth factors (IGFs) that primarily have growth functions and preferentially bind IGF receptors (IGFRs) that are structurally similar to the IR, and (3) relaxins that are vasodilators and also have other functions mediated by binding to specific G protein-coupled receptors (GPCRs) (McDonald et al., 1989; Murray-Rust et al., 1992; De Meyts, 2004; Halls et al., 2007). Vertebrate immune cells express IGFRs and downstream components of IGF signaling that promote lymphopoiesis, erythropoiesis and thymic development (Clark, 1997; Miyagawa et al., 2000). Misregulation of IGF signaling in T cells has also been implicated in pro-inflammatory autoimmune disorders such as encephalomyelitis (Delgoffe et al., 2011; DiToro et al., 2020). This brief summation of the vertebrate literature is pertinent to the current study because mosquitoes and other insects encode multiple ILPs but differ because most species encode only one IR-IGFR-like RTK, usually referred to as the IR, plus one or two relaxin-like GPCRs, while no ILP family members are known to exhibit distinct insulin versus IGF functions (Teleman, 2010; Vogel et al., 2013; Nassel et al., 2015; Strand et al., 2016). Thus, insect ILPs differ from vertebrates in that family members such as ILP3 from *Ae. aegypti* have both insulin and IGF-like growth functions that are transduced through binding to a single IR-like receptor (Brown et al., 2008; Wen et al., 2010). The metabolic and growth functions of ILP3 further vary by cell or tissue type, with results from this study showing that ILP3 stimulates hemocytes to proliferate and earlier results showing that ILP3 also stimulates follicle cells to proliferate (Valzania et al., 2019) while concurrently affecting metabolism in these cells types as well as others such as fat body cells (Brown et al., 2008; Wen et al., 2010).

The primary known function of OEH is to stimulate ovary follicle cells to produce ecdysteroids, which further depends on binding to the OEHR that also activates the IIS pathway (Brown et al., 1998; Dhara et al., 2013; Vogel et al., 2015). Dose–response assays indicate that follicle cell proliferation is most strongly induced by ILP3 but OEH also exhibits proliferation activity (e.g. Valzania et al., 2019). When combined with findings from this study, we conclude that ILP3 is the primary factor that stimulates two cell types, ovary follicle cells and hemocytes, to proliferate during a gonadotrophic cycle. We also hypothesize that ovary follicle cells proliferate in response to both ILP3 and OEH because the IR and OEHR are both strongly expressed in this cell type. In contrast, results reported here indicate that the IR is much more strongly expressed than the OEHR in hemocytes, which potentially underlies why ILP3 but not OEH stimulates hemocyte proliferation. While most mosquito hemocytes are in circulation, estimates from *An. gambiae* indicate a quarter of the population is sessile and attached to tissues that include the dorsal vessel (King and Hillyer, 2013). Thus, it is possible that the increase in circulating hemocytes that occurs in response to ILP3 could also involve sessile hemocytes entering circulation.

Prior studies have identified a number of immune genes that are expressed in hemocytes as well as many other genes that serve as markers for different hemocyte types (Baton et al., 2009; Pinto et al., 2009; Severo et al., 2018; Raddi et al., 2020; Kwon et al., 2021). Results from the present study strongly support that ILP3 stimulates hemocytes to proliferate by activating the IIS pathway. We thus conclude that ILP3 increases the number of hemocytes in circulation after a blood meal, which potentially enables females to more strongly respond to invading pathogens. In contrast, immune genes that encode effector molecules such as antimicrobial peptides are not transcriptionally upregulated. We hypothesize that the absence of immune gene upregulation is likely an adaptation toward minimizing inflammatory responses that could otherwise damage mosquito tissues as occurs in certain vertebrate autoimmune disorders when IGF-mediated functions are misregulated (DiToro et al., 2020). Our results also indicate that 20E does not stimulate hemocyte proliferation, but the increase in 20E titer that occurs after blood feeding could complement the increase in hemocyte abundance by promoting phagocytosis if pathogens are encountered as reported in both *An. gambiae* and *Drosophila melanogaster* (Sampson et al., 2013; Regan et al., 2013; Reynolds et al., 2020).

In contrast to hemocytes, prior studies indicate many genes with functions in metabolism, vitellogenesis and blood meal digestion are differentially expressed in the fat body after blood feeding in response to 20E, ILPs and OEH (Roy et al., 2007; Brown et al., 2008; Price et al., 2011; Akbari et al., 2013; Vogel et al., 2015; Wang et al., 2017, 2021). Notably though, previous studies have also identified few differences in the expression of immune genes in the fat body between NBF and BF *Ae. aegypti* (Price et al., 2011; Upton et al., 2015), whereas systemic infection by bacteria upregulates a number of immune genes through binding to pattern recognition receptors (PRRs) that activate immune signaling

pathways (Dimopoulos, 2003; Lemaitre and Hoffmann, 2007). Thus, it would appear that the absence of immune gene upregulation in the fat body after blood feeding is also likely an adaptation toward minimizing inflammatory responses in the absence of infection. Certain immune genes in the *Ae. aegypti* gut are differentially detected between NBF and BF females (Dong et al., 2017). Unlike the fat body though, gut cells express PRRs that are in continuous contact with bacteria in the gut lumen that comprise the gut microbiota (Dong et al., 2009; Song et al., 2018; Gendrin et al., 2017; Cappelli et al., 2019). Certain bacteria in the midgut also greatly increase in abundance after a female blood feeds (Oliveira et al., 2011; Gaio et al., 2011; Coon et al., 2014), which could further affect immune gene expression and potentially influence the abundance of gut microbiota community members.

In summary, this study advances understanding of hemocyte proliferation after females blood feed by showing that ILP3 regulates this response in three obligately anautogenous species. Our comparative results further indicate that ILP3 stimulates hemocytes to increase in abundance in two facultatively autogenous species that still retain the ability to blood feed but does not affect hemocyte abundance in *T. amboinensis*, which never blood feeds. Determining whether hemocyte proliferation as a potential anticipatory defense response has been lost in other obligately autogenous species is one area for future study. Another is to better understand how increases in hemocyte abundance enhance defense when a female is infected by pathogens in a blood meal or endogenous microbes in the gut that could potentially gain entry to the hemocoel as a consequence of blood feeding.

Acknowledgements
We thank L. South for management of the mosquito cultures used in the study. We also thank J. A. Johnson for assistance with management of the mosquito cultures and photography.

Competing interests
The authors declare no competing or financial interests.

Author contributions
Conceptualization: M.R.S.; Methodology: E.O.M., K.C., L.V., M.R.B., M.R.S.; Formal analysis: E.O.M., K.C., L.V., M.R.S.; Investigation: E.O.M., K.C., L.V., M.R.B., M.R.S.; Data curation: E.O.M.; Writing - original draft: E.O.M., M.R.S.; Writing - review & editing: E.O.M., K.C., L.V., M.R.B., M.R.S.; Supervision: M.R.S.; Project administration: M.R.S.; Funding acquisition: M.R.B., M.R.S.

Funding
This work was funded by grants from the National Science Foundation (IOS 1656236 to M.R.S., M.R.B.), the National Institutes of Health (R01AI033108 to M.R.S., M.R.B.), the USDA NIFA Hatch program (GEO00772 to M.R.S.) and the Pulliam Endowment (to M.R.S.). Deposited in PMC for release after 12 months.

Data availability
The RNAseq data sets used in the study have been uploaded to the US National Center for Biotechnology Information (NCBI) as BioProject ID PRJNA752401. BioSample accessions are SRX11658639–SRX11658719.

References
Akbari, O. S., Antoshechkin, I., Amerhein, H., Williams, B., Diloreto, R., Sandler, J. and Hay, B. A. (2013). The developmental transcriptome of the mosquito *Aedes aegypti*, an invasive species and major arbovirus vector. *G3* **3**, 1493-1509. doi:10.1534/g3.113.006742

Anders, S. and Huber, W. (2010). Differential expression analysis for sequence count data. *Genome Biol.* **11**, R106. doi:10.1186/gb-2010-11-10-r106

Attardo, G. M., Hansen, I. A. and Raikhel, A. S. (2005). Nutritional regulation of vitellogenesis in mosquitoes: implications for anautogeny. *Insect Biochem. Mol. Biol.* **35**, 661-675. doi:10.1016/j.ibmb.2005.02.013

Baldini, F., Gabrieli, P., South, A., Valim, C., Mancini, F. and Catteruccia, F. (2013). The interaction between a sexually transferred steroid hormone and a female protein regulates oogenesis in the malaria mosquito *Anopheles gambiae*. *PLoS Biol.* **11**, e1001695. doi:10.1371/journal.pbio.1001695

Baton, L. A., Robertson, A., Warr, E., Strand, M. R. and Dimopoulos, G. (2009). Genome-wide transcriptomic profiling of *Anopheles gambiae* hemocytes reveals pathogen-specific signatures upon bacterial challenge and *Plasmodium berghei* infection. *BMC Genomics* **10**, 257. doi:10.1186/1471-2164-10-257

Bertone, M. A., Courtney, G. W. and Wiegmann, B. M. (2008). Phylogenetics and temporal diversification of the earliest true flies (Insecta: Diptera) based on multiple nuclear genes. *Sys. Entomol.* **33**, 668-687. doi:10.1111/j.1365-3113.2008.00437.x

Blandin, S. A. and Levashina, E. A. (2007). Phagocytosis in mosquito immune responses. *Immunol. Revs.* **219**, 8-16. doi:10.1111/j.1600-065X.2007.00553.x

Bradshaw, W. E., Burkhart, J., Colbouurne, J. K., Borowczak, R., Lopez, J., Denlinger, D. L., Reynolds, J. A., Pfrender, M. E. and Holzapfel, C. M. (2018). Evolutionary transition from blood feeding to obligate nonbiting in a mosquito. *Proc. Nat.l Acad. Sci. USA* **115**, 1009-1014. doi:10.1073/pnas.1717502115

Briegel, H. (2003). Physiological bases of mosquito ecology. *J. Vector Ecol.* **28**, 1-11.

Brown, M. R. and Cao, C. (2001). Distribution of ovary ecdysteroidogenic hormone I in the nervous system and gut of mosquitoes. *J. Insect Sci.* **1**, 1-3. doi:10.1673/031.001.0301

Brown, M. R., Graf, R., Swiderek, K. M., Fendley, D., Stracker, T. H., Champagne, D. E. and Lea, A. O. (1998). Identification of a steroidogenic neurohormone in female mosquitoes. *J. Biol. Chem.* **273**, 3967-3971. doi:10.1074/jbc.273.7.3967

Brown, M. R., Clark, K. D., Gulia, M., Zhao, Z., Garczynski, S. F., Crim, J. W., Suderman, R. J. and Strand, M. R. (2008). An insulin-like peptide regulates egg maturation and metabolism in the mosquito Aedes aegypti. *Proc. Natl. Acad. Sci. USA* **115**, 5716-5721. doi:10.1073/pnas.0800478105

Bryant, W. B. and Michel, K. (2014). Blood feeding induces hemocyte proliferation and activation in the African malaria mosquito, *Anopheles gambiae* Giles. *J. Exp. Biol.* **217**, 1238-1245. doi:10.1242/jeb.094573

Bryant, W. B. and Michel, K. (2016). *Anopheles gambiae* hemocytes exhibit transient states of activation. *Dev. Comp. Immunol.* **55**, 119-129. doi:10.1016/j.dci.2015.10.020

Cappelli, A., Damiani, C., Mancini, M. V., Valzano, M., Rossi, P., Serrao, A., Ricci, I. and Favia, G. (2019). *Asaia* activates immune genes in mosquito eliciting an anti-*Plasmodium* response: implications in malaria control. *Front. Genet.* **10**, 836. doi:10.3389/fgene.2019.00836

Castillo, J., Robertson, A. and Strand, M. R. (2006). Characterization of hemocytes from the mosquitoes *Anopheles gambiae* and *Aedes aegypti*. *Insect Biochem. Mol. Biol.* **6**, 891-903. doi:10.1016/j.ibmb.2006.08.010

Castillo, J., Brown, M. R. and Strand, M. R. (2011). Blood feeding and insulin-like peptide 3 stimulate proliferation of hemocytes in the mosquito *Aedes aegypti*. *PLoS Path.* **7**, e1002274. doi:10.1371/journal.ppat.1002274

Clark, R. (1997). The somatogenic hormones and insulin-like growth factor-1: stimulators of lymphopoiesis and immune function. *Endocr. Rev.* **18**, 157-179. doi:10.1210/edrv.18.2.0296

Clements, A. N. (1992). *The Biology of Mosquitoes: Development, Nutrition and Reproduction*, Vol. 1. Chapman & Hall.

Coon, K. L., Vogel, K. J., Brown, M. R. and Strand, M. R. (2014). Mosquitoes rely on their gut microbiota for development. *Mol. Ecol.* **23**, 2727-2739. doi:10.1111/mec.12771

Coon, K. L., Valzania, L., Brown, M. R. and Strand, M. R. (2020). Predaceous *Toxorhynchites* mosquitoes require a living gut microbiota to develop. *Proc. R. Soc. B* **287**, 20192705. doi:10.1098/rspb.2019.2705

Delgoffe, G. M., Pollizzi, K. N., Waickman, A. T., Heikamp, E., Meyers, D. J., Horton, M. R., Xiao, B., Worley, P. F. and Powell, J. D. (2011). The kinase mTOR regulates the differentiation of helper T cells through the selective activation of signaling by mTORC1 and mTORC2. *Nat. Immunol.* **12**, 295-303. doi:10.1038/ni.2005

De Meyts, P. (2004). Insulin and its receptor: structure, function and evolution. *BioEssays* **26**, 1351-1362. doi:10.1002/bies.20151

Dhara, A., Eum, J.-H., Robertson, A., Gulia-Nuss, M., Vogel, K. J., Clark, K. D., Graf, R., Brown, M. R. and Strand, M. R. (2013). Ovary ecdysteroiogenic hormone functions independently of the insulin receptor in the yellow fever mosquito, *Aedes aegypti*. *Insect Biochem. Mol. Biol.* **43**, 1100-1108. doi:10.1016/j.ibmb.2013.09.004

Dimopoulos, G. (2003). Insect immunity and its implications in mosquito–malaria interactions. *Cell. Microbiol.* **5**, 3-14. doi:10.1046/j.1462-5822.2003.00252.x

DiToro, D., Harbour, S. N., Bando, J. K., Benavides, G., Witte, S., Laufer, V. A., Moseley, C., Singer, J. R., Fey, B., Turner, H. et al. (2020). Insulin-like growth factor are key regulators of T helper 17 regulatory T cell balance in autoimmunity. *Immunity* **52**, 650-667. doi:10.1016/j.immuni.2020.03.013

Donald, C. L., Siriyasatien, P., Kohl, A. (2020). *Toxorhynchites* species: a review of current knowledge. *Insects* **11**, 11110747. doi:10.3390/insects11110747

Dong, Y., Manfredini, F. and Dimopoulos, G. (2009). Implication of the mosquito midgut microbiota in the defense against malaria parasites. *PLoS Path.* **5**, e1000423. doi:10.1371/journal.ppat.1000423

Dong, S., Behura, S. K. and Franz, A. W. E. (2017). The midgut transcroptome of *Aedes aegypti* fed with saline or protein meals containing chikungunya virus reveals genes potentially involved in viral midgut escape. *BMC Genomics* **18**, 382. doi:10.1186/s12864-017-3775-6

Fernandes, L. and Briegel, H. (2005). Reproductive physiology of *Anopheles gambiae* and *Anopheles atroparvus*. *J. Vector Ecol.* **30**, 11-26.
Foster, W. A. and Lea, A. O. (1975). Renewable fecundity of male *Aedes aegypti* following replenishment of seminal vesicles and accessory glands. *J. Insect Physiol.* **21**, 1085-1090. doi:10.1016/0022-1910(75)90120-1
Gaio, A. D., Gusmão, D. S., Santos, A. V., Berbert-Molina, M. A., Pimenta, P. F. P. and Lemos, F. J. A. (2011). Contribution of midgut bacteria to blood digestion and egg production in *Aedes aegypti* (Diptera: Culicidae) (L.). *Parasites Vectors* **4**, 105. doi:10.1186/1756-3305-4-105
Gao, Q., Su, F., Zhou, Y.-B., Chu, W., Cao, H., Song, L.-L., Zhou, J.-J. and Leng, P.-E. (2019). Autogeny, fecundity and other life history traits of *Culex pipiens molestus* (Diptera: Culicidae) in Shanghai, China. *J. Med. Ent.* **56**, 656-664. doi:10.1093/jme/tjy228
Gendrin, M., Turlure, F., Rodgers, F. H., Cohuet, A., Morlais, I. and Christophides, G. K. (2017). The peptidoglycan recognition proteins PGRPLA and PGRPLB regulate *Anopheles* immunity to bacteria and affect infection by *Plasmodium*. *J. Innate Immun.* **9**, 333-342. doi:10.1159/000452797
Gulia-Nuss, M., Eum, J.-H., Strand, M. R. and Brown, M. R. (2012). Ovary ecdysteroidogenic hormone activates egg maturation in the mosquito *Georgecraigius atropalpus* after adult eclosion or a blood meal. *J. Exp. Biol.* **215**, 3758-3767. doi:10.1242/jeb.074617
Halls, M. L., van der Westhuizen, E. T., Bathgate, R. A. D. and Summers, R. J. (2007). Relaxin family peptide receptors – former orphans reunite with their parent ligands to activate multiple signalling pathways. *Brit. J. Pharmacol.* **150**, 677-691. doi:10.1038/sj.bjp.0707140
Harbach, R. E. and Kitching, I. J. (1998). Phylogeny and classification of the Culicidae (Diptera). *System. Entomol.* **23**, 327-370. doi:10.1046/j.1365-3113.1998.00072.x
Harrison, R. E., Brown, M. R. and Strand, M. R. (2021). Whole blood and blood components from vertebrates differentially affect egg formation in three species of anautogenous mosquitoes. *Parasites Vectors* **14**, 1-19. doi:10.1186/s13071-021-04594-9
Hillyer, J. F. and Strand, M. R. (2014). Mosquito hemocyte-mediated immune responses. *Curr. Op. Insect Sci.* **3**, 14-21. doi:10.1016/j.cois.2014.07.002
Kassim, N. F., Webb, C. E. and Russell, R. C. (2012). Is the expression of autogeny by *Culex molestus* Forskal (Diptera: Culicidae) influenced by larval nutrition or by adult mating, sugar feeding, or blood feeding? *J. Vector Ecol.* **3**, 162-171. doi:10.1111/j.1948-7134.2012.00213.x
King, J. G. and Hillyer, J. F. (2013). Spatial and temporal in vivo analysis of circulating and sessile immune cells in mosquitoes: hemocyte mitosis following infection. *BMC Biol.* **11**, 55. doi: 10.1186/1741-7007-11-55
Krieger, M. J. B., Jahan, N., Riehle, M. A., Cao, C. and Brown, M. R. (2004). Molecular characterization of insulin–like peptide genes and their expression in the African malaria mosquito, *Anopheles gambiae*. *Insect Mol. Biol.* **13**, 305-315. doi:10.1111/j.0962-1075.2004.00489.x
Kwon, H., Mohammed, M., Franzen, O., Ankarklev, J. and Smith, R. C. (2021). Single-cell analysis of mosquito hemocytes identifies signatures of immune cell subtypes and cell differentiation. *eLife* **10**, e66192. doi:10.7554/eLife.66192
Lemaitre, B. and Hoffmann, J. (2007). The host defense of *Drosophila melanogaster*. *Annu. Rev. Immunol.* **25**, 697-743. doi:10.1146/annurev.immunol.25.022106.141615
Li, H. and Durbin, R. (2010). Fast and accurate long-read alignment with Burrows–Wheeler transform. *Bioinformatics* **26**, 589-595. doi:10.1093/bioinformatics/btp698
McDonald, N., Murray-Rust, J. and Blundell, T. (1989). Structure–function relationships of growth factors and their receptors. *Brit. Med. Bull.* **45**, 554-569. doi:10.1093/oxfordjournals.bmb.a072342
Merritt, R. W., Dadd, R. H. and Walker, E. D. (1992). Feeding behavior, natural food, and nutritional relationships of larval mosquitoes. *Annu. Rev. Entomol.* **37**, 349-374. doi:10.1146/annurev.en.37.010192.002025
Miyagawa, S., Kobayashi, M., Konishi, N., Sato, T. and Ueda, K. (2000). Insulin and insulin-like growth factor I support the proliferation of erythroid progenitor cells in bone marrow through the sharing of receptors. *Br. J. Haematol.* **109**, 555-562. doi:10.1046/j.1365-2141.2000.02047.x
Muller, H. M., Dimopoulos, G., Blass, C. and Kafatos, F. C. (1999). A hemocyte-like cell line established from the malaria vector *Anopheles gambiae*. *J. Biol. Chem.* **274**, 11727-11735. doi:10.1074/jbc.274.17.11727
Murray-Rust, J., McLeod, A. N. and Blundell, T. L. (1992). Structure and evolution of insulins: implications for receptor binding. *BioEssays* **14**, 325-331. doi:10.1002/bies.950140507
Nassel, D. R., Liu, Y. and Luo, J. (2015). Insulin/IGF signaling and its regulation in *Drosophila*. *Gen. Comp. Endocrinol.* **221**, 255-266. doi:10.1016/j.ygcen.2014.11.021
Nuss, A. B., Brown, M. R., Murty, U. S. and Gulia-Nuss, M. (2018). Insulin receptor knockdown blocks filarial parasite development and alters egg production in the southern house mosquito, *Culex quinquefasciatus*. *PLoS Negl. Trop. Dis.* **12**, e0006413. doi:10.1371/journal.pntd.0006413
Oliveira, J. H. M., Goncalves, R. L. S., Lara, F. A., Dias, F. A., Gandara, A. C. P., Menna-Barreto, R. F. S., Edwards, M., Laurindo, F. R. M., Silva-Neto, M. A. C., Sorgine, M. H. F. et al. (2011). Blood meal-derived heme decreases ROS levels in the midgut of *Aedes aegypti* and allows proliferation of intestinal microbiota. *PLoS Path.* **7**, 1001320. doi:10.1371/journal.ppat.1001320
O'Meara, G. F. (1985). Gonotrophic interactions in mosquitoes: kicking the blood-feeding habit. *Fla. Entomol.* **68**, 122-133. doi:10.2307/3494335
Pakpour, N., Corby-Harris, V., Green, G. P., Smithers, H. M., Cheung, K. W., Riehle, M. A. and Luckhart, S. (2012). Ingested human insulin inhibits the mosquito NF-κB-dependent immune response to *Plasmodium falciparum*. *Infect. Immun.* **80**, 2141-2149. doi:10.1128/IAI.00024-12
Pearson, W. R., Wood, T., Zhang, Z. and Miller, W. (1997). Comparison of DNA sequences with protein sequences. *Genomics* **46**, 24-36. doi:10.1006/geno.1997.4995
Pinto, S. B., Lombardo, F., Koutsos, A. C., Waterhouse, R. M., McKay, K., An, C., Ramakrisnan, C., Kafatos, F. C. and Michel, K. (2009). Discovery of *Plasmodium* modulators by genome-weide analysis of circulating hemocyes in *Anopheles gambiae*. *Proc. Natl. Acad. Sci. USA* **106**, 21270-21275. doi:10.1073/pnas.0909463106
Pondeville, E., Maria, A., Jacques, J.-C., Bourgouin, C. and Dauphin-Villemant, C. (2008). *Anopheles gambiae* males produce and transfer the vitellogenic steroid hormone 20-hydroxyecdysone to females during mating. *Proc. Natl. Acad. Sci. USA* **105**, 19631-19636. doi:10.1073/pnas.0809264105
Powell, J. R. and Tabachnick, W. J. (2013). History of domestication and spread of *Aedes aegypti*: a review. *Mem. Inst. Oswaldo Cruz* **108** Suppl. 1, 11-17. doi:10.1590/0074-0276130395
Price, D. P., Nagarajan, V., Churbanov, A., Houde, P., Milligan, B., Drake, L. L., Gustafson, J. E. and Hansen, I. A. (2011). The fat body transcriptomes of he yellow fever mosquito *Aedes aegypti* pre- and post-blood meal. *PLoS ONE* **6**, e22573. doi:10.1371/journal.pone.0022573
Provost-Javier, K. N., Chen, S. and Rasgon, J. L. (2010). Vitellogenin expression in autogenous *Culex tarsalis*. *Insect Mol. Biol.* **19**, 423-429. doi:10.1111/j.1365-2583.2010.00999.x
Raddi, G., Barletta, A. B. F., Efremova, M., Ramirez, J. L., Cantera, R., Teichmann, S. A., Barillas-Mury, C. and Billker, O. (2020). Mosquito cellular immunity at single-cell resolution. *Science* **369**, 1128-1132. doi:10.1126/science.abc0322
Regan, J. C., Brandão, A. S., Leitão, A. B., Dias, R. M., Sucena, É., Jacinto, A. and Zaidman-Rémy, A. (2013). Steroid hormone signaling is essential to regulate innate immune cells and fight bacterial infection in *Drosophila*. *PLoS Pathog.* **9**, e1003720. doi:10.1371/journal.ppat.1003720
Reidenbach, K. R., Cook, S., Bertone, M. A., Harbach, R. E., Wiegmann, B. M. and Besansky, N. J. (2009). Phylogenetic analysis and temporal diversification of mosquitoes (Diptera: Culicidae) based on nuclear genes and morphology. *BMC Evol. Biol.* **9**, 298. doi:10.1186/1471-2148-9-298
Reynolds, R. A., Kwon, H. and Smith, R. C. (2020). 20-Hydroxyecdysone primes innate immune responses that limit bacterial and malarial parasite survival in *Anopheles gambiae*. *mSphere* **5**, e00983-e00919. doi:10.1128/mSphere.00983-19
Rioux, J. A., Crost, H., Pech-Perieres, J., Guilvard, E. and Belmonte, A. (1975). L 'autogénèse chez les diptères autogénes. *Ann. Parasit. Hum. Comp.* **50**, 134-140. doi:10.1051/parasite/1975501134
Roubaud, E. (1929). Cycle autogene d'attente generations hivernales suractives inaparentes chez le moustique commun *Culex pipiens*. *C. R. Acad. Sci. Paris* **180**, 735-738.
Roy, S. G., Hansen, I. A. and Raikhel, A. S. (2007). Effect of insulin and 20-hydroxyecdysone in the fat body of the yellow fever mosquito, *Aedes aegypti*. *Insect Biochem. Mol. Biol.* **37**, 1317-1326. doi:10.1016/j.ibmb.2007.08.004
Sampson, C. J., Amin, U. and Couso, J.-P. (2013). Activation of *Drosophila* hemocyte motlity by the ecdysone hormone. *Biol. Open* **15**, 1412-1420. doi:10.1242/bio.20136619
Severo, M. S., Landry, J. J., Lindquist, R. L., Goosmann, C., Brinkmann, V., Collier, P., Hauser, A. E., Benes, V., Henriksson, J., Teichmann, S. A. et al. (2018). Unbiased classification of mosquito blood cells by single-cell genomics and high-content imaging. *Proc. Natl. Acad. Sci. USA* **115**, E7568-E7577. doi:10.1073/pnas.1803062115
Song, X., Wang, M., Dong, L., Zhu, H. and Wang, J. (2018). PGRP-LD mediates *A. stephensi* vector competency by regulating homeostasis of microbiota induced peritrophic matrix synthesis. *PLoS Pathog.* **14**, e1006899. doi:10.1371/journal.ppat.1006899
Strand, M. R., Brown, M. R. and Vogel, K. J. (2016). Mosquito peptide hormones: diversity, production, and function. *Adv. Insect Physiol.* **51**, 145-188. doi:10.1016/bs.aiip.2016.05.003
Teleman, A. A. (2010). Molecular mechanisms of metabolic regulation by insulin in *Drosophila*. *Biochem. J.* **425**, 13-26. doi:10.1042/BJ20091181
Trapnell, C., Williams, B. A., Pertea, G., Mortazavi, A., Kwan, G., van Baren, M. J., Salzberg, S. L., Wold, B. J. and Pachter, L. (2010). Transcript assembly and quantification by RNA-Seq reveals unannotated transcripts and isoform switching during cell differentiation. *Nat. Biotechnol.* **28**, 511-515. doi:10.1038/nbt.1621
Tsuji, N., Okazawa, T. and Yamaura, N. (1990). Autogenous and anautogenous mosquitoes. *J. Med. Entomol.* **27**, 446-453. doi:10.1093/jmedent/27.4.446

Upton, L. M., Povelones, M. and Christophides, G. K. (2015). *Anopheles gambiae* blood feeding initiates an anticipatory defense response to *Plasmodium berghei*. *J. Innate Immun.* **7**, 74-86. doi:10.1159/000365331

Valzania, L., Mattee, M. T., Strand, M. R. and Brown, M. R. (2019). Blood feeding activates the vitellogenic stage of oogenesis in the mosquito *Aedes aegypti* through inhibition of glycogen synthase kinase 3 by the insulin and TOR pathways. *Dev. Biol.* **454**, 85-95. doi:10.1016/j.ydbio.2019.05.011

Vogel, K. J., Brown, M. R. and Strand, M. R. (2013). Phylogenetic investigation of peptide hormone and growth factor receptors in five dipteran genomes. *Front. Endocrinol.* **4**, 193. doi:10.3389/fendo.2013.00193

Vogel, K. J., Brown, M. R. and Strand, M. R. (2015). Ovary ecdysteroidogenic hormone requires a receptor tyrosine kinase to activate egg formation in the mosquito *Aedes aegypti*. *Proc. Natl. Acad. Sci. USA* **112**, 5057-5062. doi:10.1073/pnas.1501814112

Wang, X., Hou, Y., Saha, T. T., Pei, G., Raikhel, A. S. and Zou, Z. (2017). Hormone and receptor interplay in the regulation of mosquito lipid metabolism. *Proc. Natl. Acad. Sci. USA* **114**, E2709-E2718. doi:10.1073/pnas.1619326114

Wang, X., Ding, Y., Lu, X., Geng, D., Li, S., Raikhel, A. S. and Zou, Z. (2021). The ecdysone-induced protein 93 is a key factor in the adult female mosquito *Aedes aegypti*. *Proc. Natl. Acad. Sci. USA* **118**, e2021910118. doi:10.1073/pnas.2021910118

Wen, Z., Gulia, M., Clark, K. D., Dhara, A., Crim, J. W., Strand, M. R. and Brown, M. R. (2010). Two insulin-like peptide family members from the mosquito *Aedes aegypti* exhibit differential biological and receptor binding activities. *Mol. Cell Endocrinol.* **328**, 47-55. doi:10.1016/j.mce.2010.07.003

Yee, D. A., Kesavaraju, B. and Juliano, S. A. (2007). Direct and indirect effects of animal detritus on growth, survival and mass of invasive container mosquito *Aedes albopictus* (Diptera: Culicidae). *J. Med. Ent.* **44**, 580-588. doi:10.1093/jmedent/44.4.580

A

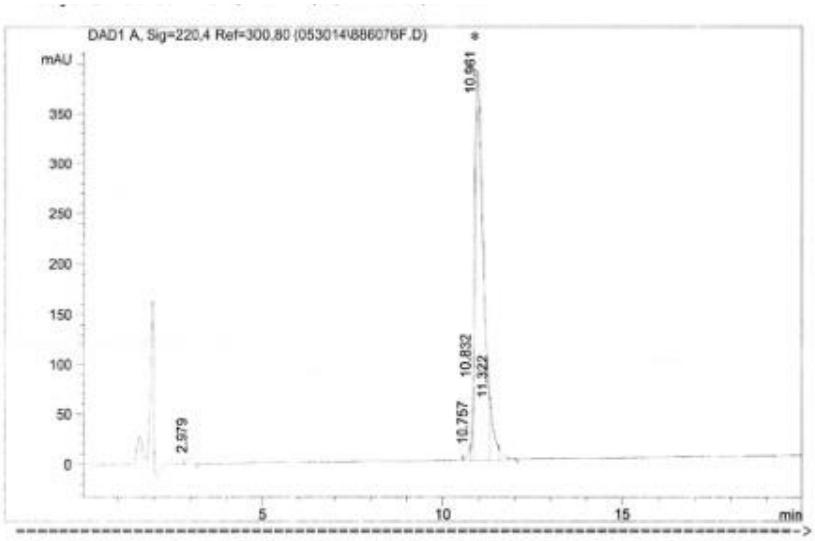

B

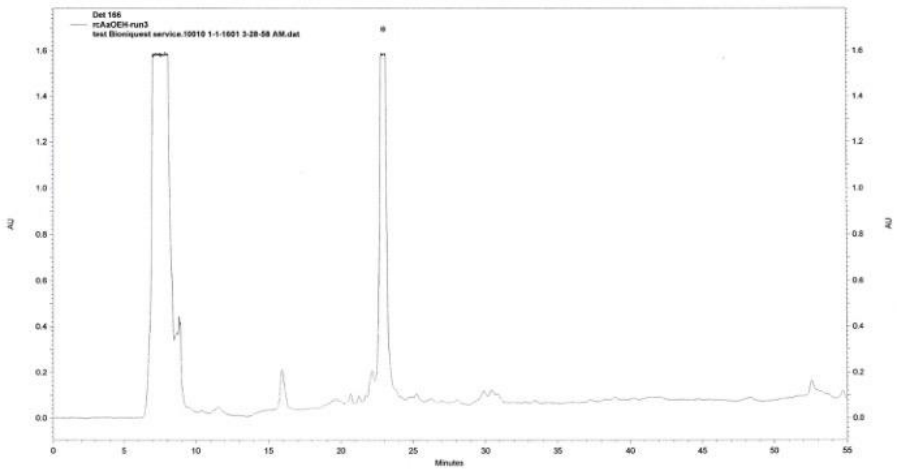

Fig. S1. Chromatograms showing the purification of ILP3 (A) and OEH (B). (A) After synthesis, ILP3 was purity checked by elution on a reversed phase column (Phenomenex Jupiter C18 (5 µµm, 120 Å) 4.6 X 150 mm) with a gradient of solvents A (0.1% TFA in HPLC water) and B (0.1% TFA in 80% acetonitrile and 10% water). ILP3 eluted as single peak as indicated by an asterisk (*) at 10-11 min with the gradient program (33 – 63% solvent B for 20 min, 1 ml/min flow) as monitored at 220 nm. (B) Recombinant OEH (18,278 MW) produced in *E. coli* was extracted in 0.5 ml of denaturing buffer (50 mM Tris pH 8.0, 0.2 M NaCl, 2 mM EDTA, and 7 M GuHCl) for 1 h at room temperature. Solvent (0.5 ml of 20% acetonitrile/80% water with 0.1% trifluoroacetic acid (TFA)) was added, and after mixing, 0.1 ml was added to 0.5 ml of the same solvent, mixed, and centrifuged (13K x g, 4 min). The supernatant was injected onto a reversed phase column (Phenomenex Jupiter C18 (5 µm, 300Å) 10 X 220 mm), which eluted as a single peak as indicated by an asterisk (*) at 23-24 min with a gradient of solvents A (0.1% TFA in HPLC water) and B (0.1% TFA in 90% acetonitrile and 10% water). The gradient program was set with a flow of 2 ml/min and monitored at 220 nm: solvent B 20%, 5 min; 20 - 50%, 10 min; 50 - 70%, 30 min; 70 – 100%, 5 min; 100 – 20%, 5 min. Fractions of this peak were then pooled, lyophilized, and stored at -80°C. Weighed portions were prepared as a 200 pmol/ul stock in pure water, aliquoted, and stored at -80° C for use one time.

Table S1. The expression in FPKM of the 548 genes identified by Raddi et al. (2020) as hemocyte markers averaged over three replicates of hemocytes . BF, expression measured 24h after blood feeding; NBF, expression measured in age-match non-blood fed mosquitoes; ILP3; expression measured 24 h after blood feeding, decapitation, and ILP3 injection.

Click here to download Table S1

Table S2. Genes with FPKM =10 identified in hemocytes from age-matched NBF females, BF females 24 h PBM, or BF females 24 h PBM that were injected with ILP3 and decapitated. Each row indicates the gene, average FPKM across the three replicate libraries for each treatment with an X indicating expression exceeded a 10 FPKM cutoff.

Click here to download Table S2

Table S3. Gene ontology (GO) terms identified among the 262 genes that were preferentially expressed with FPKM=10 in hemocytes from BF females that were injected with ILP3 and decapitated.

Click here to download Table S3

Table S4. Genes with FPKM values =10 in in three replicates of hemocytes from BF females 24 h PBM that were injected with ILP3 and decapitated, age-matched NBF females, and BF females 24 h PBM. Significanly differentially expressed genes between only ILP3 and NBF females, only ILP3 and BF females, and ILP3 to both NBF and BF females are denoted with an "X" .

Click here to download Table S4

Table S5. The expression in FPKM of immune genes averaged over three replicates of hemocytes . BF, expression measured 24h after blood feeding; NBF, expression measured in age-match non-blood fed mosquitoes; ILP3; expression measured 24 h after blood feeding, decapitation, and ILP3 injection.

Click here to download Table S5